Marine and Petroleum Geology 178 (2025) 107424

Contents lists available at ScienceDirect

Marine and Petroleum Geology

journal homepage: www.elsevier.com/locate/marpetgeo

A new method for identification of effective hydrocarbon source rocks and evaluation of relative contributions to reservoirs

Huiyi Xiao [a,b], Tao Hu [a,b,*], Xiongqi Pang [a,b,**], Yunlong Xu [c], Yao Hu [a,b], Caijun Li [a,b], Tianwu Xu [c], Dingye Zheng [d], Tingyu Pu [a,b], Chenxi Ding [b], Zhiming Xiong [a,b], Shu Jiang [e], Kanyuan Shi [a,b], Qinglong Lei [a,b], Yuqi Wu [a,b], Maowen Li [d]

[a] State Key Laboratory of Petroleum Resources and Engineering, China University of Petroleum (Beijing), Beijing, 102249, China
[b] College of Geosciences, China University of Petroleum (Beijing), Beijing, 102249, China
[c] Exploration and Development Research Institute, Zhongyuan Oilfield Company, SINOPEC, Puyang, 457001, China
[d] Exploration and Development Research Institute, SINOPEC, Beijing, 100083, China
[e] Key Laboratory of Tectonics and Petroleum Resources, China University of Geosciences, Ministry of Education, Wuhan, 434100, China

ARTICLE INFO

Keywords:
Effective hydrocarbon source rock
Data-driven simulation
Micromigration
Hydrocarbon generation kinetics
Resource evaluation

ABSTRACT

Previous resource evaluation methods failed to consider the genetic relationships among conventional and unconventional reservoirs. In particular, the boundary between shale as source rock or reservoir is unclear. A unified evaluation method was developed for oil and gas. Initially, hydrocarbon micromigration in shale was evaluated to identify effective source rocks. Then, a mass-conservation model was developed based on hydrocarbon generation kinetics through Monte Carlo simulations. The model was then used for the Dongpu Depression of the Bohai Bay Basin, China. The results showed that effective source rocks capable of expelling hydrocarbons account for 62 % of the total shale count. The average original hydrocarbon generation potential index of source rocks was 490 mg/g, with hydrocarbon generation threshold of 0.37 % Ro and expulsion threshold of 0.68 % Ro, with peak hydrocarbon generation and expulsion rates being 0.8 % and 1.2 % Ro. The direct use of the uncalibrated pyrolysis data has certain limitations. For example, an S1 loss reaching up to 53 % is possible. Neglecting the mass and TOC loss of organic-rich rock could make the resource underestimate greater than 20 %. In this study, shale and tight sandstone reservoirs are defined as unconventional reservoirs. Notably, 59 % of the expelled hydrocarbons experience micromigration and are retained within the shale sequence. The generated hydrocarbons are distributed 81.1 % in shale, 14.4 % in tight sandstones reservoirs, and 4.5 % in conventional reservoirs. This study provides an easy-to-use method for the classification and joint evaluation of hydrocarbon resources, which can be applied worldwide to reduce exploration risk. The evaluation of hydrocarbon volumes in shale systems, along with the impact of heterogeneity on these estimates, requires a sustained and focused effort.

1. Introduction

Hydrocarbons originate through the thermal evolution of organic matter of sedimentary rocks, and undergo various migration processes into reservoirs. Oil and gas reserve assessments using volumetric and mass balance approaches involve multiple rounds of evaluation. For example, conventional oil resources (2071×10^9 bbls) far exceed the resources of shale (tight) oil (531×10^9 bbls) (IEA, 2023), the latter require fracturing in order to be extracted (Masters, 1979), whereas the former usually undergoes relatively distant migration and accumulates in specific traps (Magoon and Dow, 1991). Previous evaluations were limited to specific conventional or unconventional hydrocarbons, making it impossible to accurately determine how much of the different types of hydrocarbon resources relate to each other and the total available (Zheng et al., 2019). Based on whether extraction enhancement technology is needed, hydrocarbons have been categorized as conventional and unconventional. The amount of hydrocarbon resources assessed by organizations such as the IEA are not the total hydrocarbons, as they are realistic recoverable resources that change with

* Corresponding author. State Key Laboratory of Petroleum Resources and Engineering, China University of Petroleum (Beijing), Beijing, 102249, China.
** Corresponding author. State Key Laboratory of Petroleum Resources and Engineering, China University of Petroleum (Beijing), Beijing, 102249, China.
E-mail addresses: thu@cup.edu.cn (T. Hu), pangxq@cup.edu.cn (X. Pang).

https://doi.org/10.1016/j.marpetgeo.2025.107424
Received 3 December 2024; Received in revised form 20 April 2025; Accepted 21 April 2025
Available online 21 April 2025

List of abbreviations

GPI	Generation potential index
HCI	Hydrocarbon index
HET	Hydrocarbon expulsion threshold
HGE	Hydrocarbon generation and expulsion
HGT	Hydrocarbon generation threshold
HI_{TR}	HI transformation rate
TOC	Total organic carbon
ER	Expulsion rate
TR	Transformation rate

technological advances and the discovery of new types of reservoirs (USGS, 2012; IEA, 2023).

Three main hydrocarbon-reserve assessment methods are typically used: statistical, analogy, and genetics. However, each method has its limitations. The statistical method derives objective results from a mathematical perspective based on large number of oilfields. A mature exploration state is required to provide a meaningful population. The analogy method is primarily used when exploration data is lacking to infer the resource potential of a target area based on similarities with known reservoirs. Thus, the evaluator's selection of the parameters and areas to be used for the analogy has a significant impact on the results of the evaluation (White et al., 1979). The genetic method relies on basin simulation, which involves highly complex parameters and processes. Consequently, this method requires substantial data and modeling software (Lehne and Dieckmann, 2007; Zou et al., 2014; Li et al., 2020). In addition, using traditional resource evaluation methods ignores the genetic relationships between various hydrocarbons types. Moreover, these methods do not pay sufficient attention to residual hydrocarbons. Previous studies established unified models based on the organic genesis of hydrocarbons and classified types of hydrocarbons and migration processes involved (Tissot and Espitalié, 1975; Jia et al., 2017), and it is inferred that: 1) organic-rich rocks host residual hydrocarbons that serve as shale reservoirs. 2) As organic-rich rocks mature, they release hydrocarbons into different types of reservoirs at different stages of maturation, leading to the formation of different types of hydrocarbon reservoirs. 3) Based on the physical properties of the reservoir corresponding to the time of hydrocarbon expulsion, the expelled hydrocarbons can be subdivided into conventional hydrocarbons expelled at an early stage and tight hydrocarbons expelled at a late stage, which results in two basic types of conventional reservoirs and tight reservoirs (Fig. 1).

Pang et al. (2005) proposed an evaluation method for hydrocarbon generation potential based on pyrolysis datasets; the method has been continuously improved during its application to several petroleum basins (Zheng et al., 2019; Li et al., 2020). These improvements include: (1) Calibration of source rock weight and total organic carbon (TOC) depletion during hydrocarbon generation and expulsion, as well as light hydrocarbon loss during sampling and preservation, to enhance model accuracy; (2) introduction of dynamic boundaries of hydrocarbons based on hydrocarbon accumulation dynamics to distinguish hydrocarbons of conventional and unconventional reservoirs; (3) introduction of the kerogen transformation ratio (TR) based on hydrocarbon generation kinetics to quantify residual pyrolysis hydrocarbons and free hydrocarbons; and (4) utilization of Monte Carlo simulations to recover hydrocarbon generation and expulsion (HGE) trends rather than artificially plotting envelopes of maximum value (Fig. 2a and b). Nevertheless, there is strong heterogeneity of organic-rich rock stratigraphic systems vertically and laterally, posing challenges in evaluating the HGE

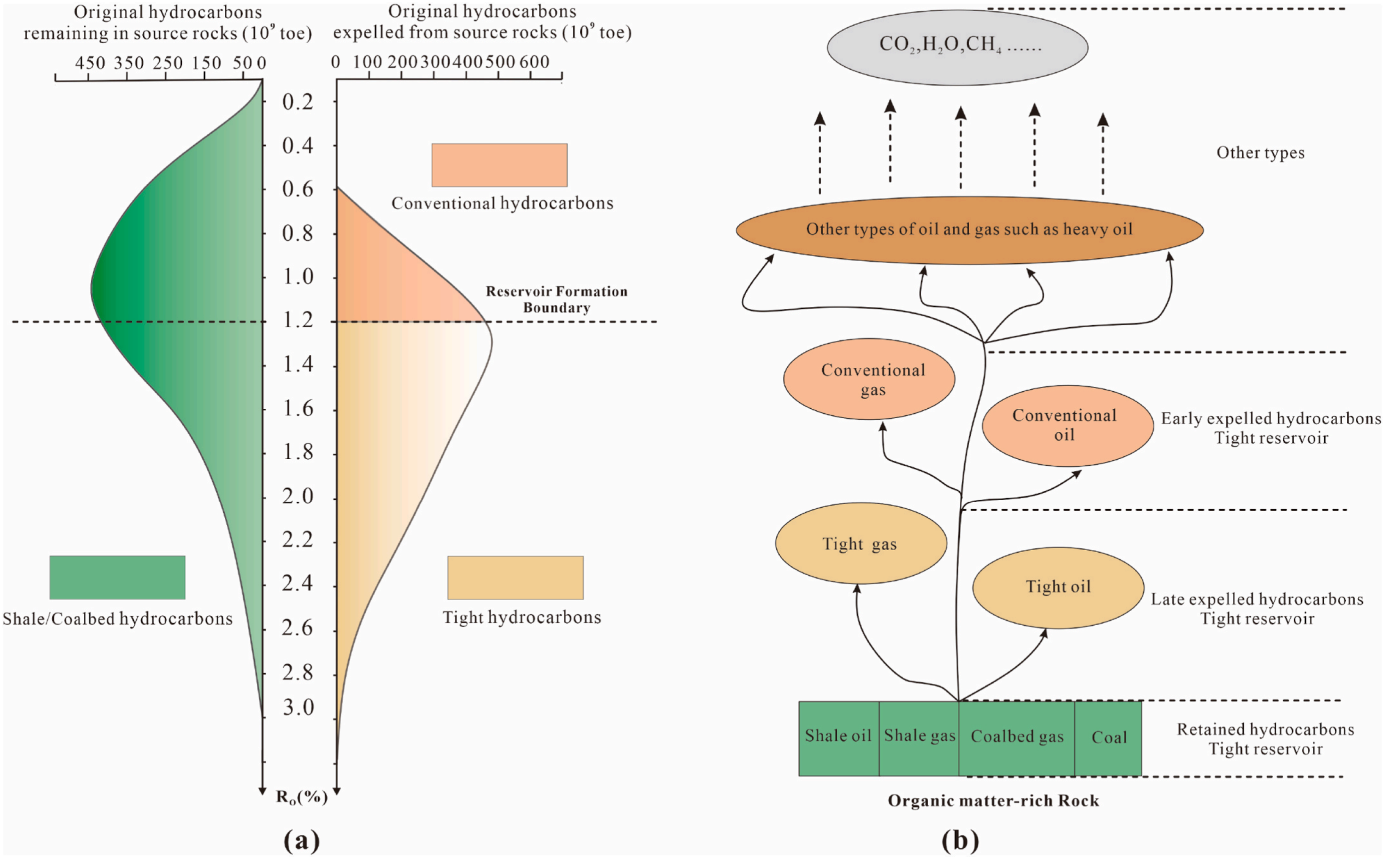

Fig. 1. Genesis and linkages of different hydrocarbons. (a) Three basic forms of hydrocarbons. Retained hydrocarbons accumulate after generation; expelled hydrocarbons are classified as conventional and tight hydrocarbons. (b)Transformation relationships of various types of hydrocarbons.

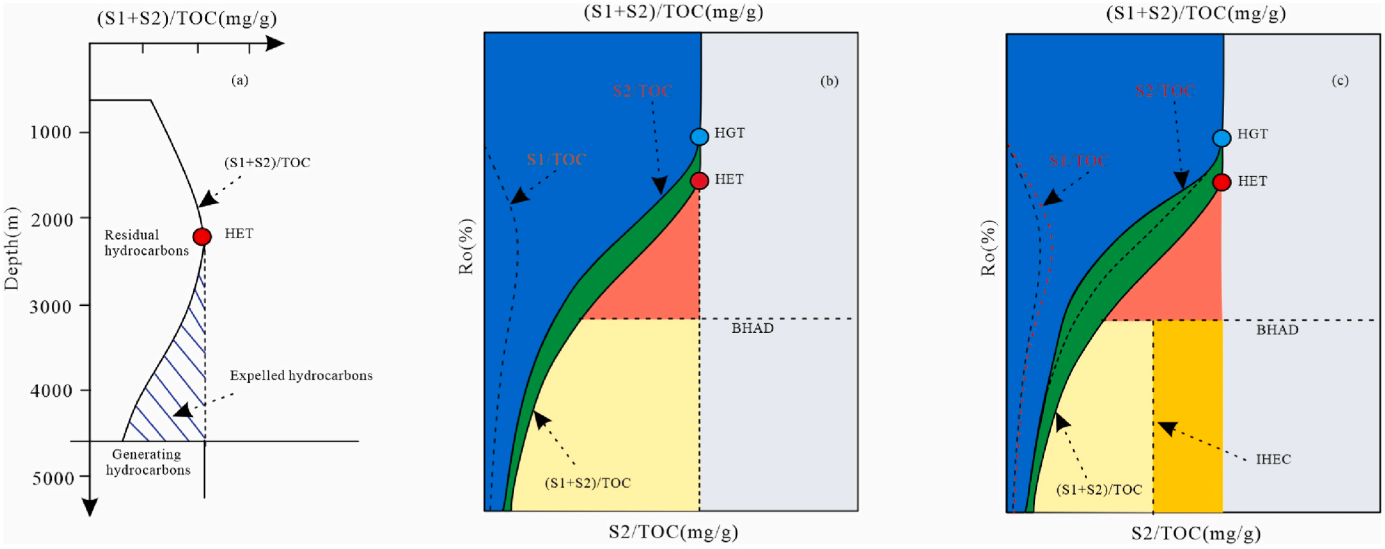

Fig. 2. Development history of the hydrocarbon generation potential model (modified from Pang et al., 2005; Li et al., 2020) (a) Original hydrocarbon generation potential model driven by data to determine the HGE trend, which can be used to distinguish residual and expelled hydrocarbons, HET-Hydrocarbon expulsion threshold. (b) Improved hydrocarbon generation potential model that incorporates calibrated parameters and hydrocarbon generation kinetics with numerical simulations to determine the HGE trend; the introduced buoyancy-driven hydrocarbon accumulation depth limit (BHAD) can distinguish conventional and tight hydrocarbons, HGT-Hydrocarbon generation threshold. (c) HGE trend calibration after excluding samples contaminated with external hydrocarbons and calibrating adsorbed hydrocarbons; the resource potential of shale hydrocarbons within the source can be determined using the internal hydrocarbon expulsion coefficient (IHEC) of each reservoir within the shale systems.

potential (Hu et al., 2018; Wang et al., 2019, 2022). Hydrocarbon migration commonly occurs within the organic-rich layer, which means that shale can can not only play the role of a source rock but also as a reservoir (Tissot and Espitalié, 1975; Jarvie, 2012; Cui et al., 2022; Hu et al., 2023, 2025). In the past, it was thought that shale was usually directly considered to be the source rock, or shale with a certain organic matter abundance could be used as the source rock, and it is inappropriate to use non-source rocks that do not expel hydrocarbons in the construction of HGE models. In addition to expelling hydrocarbons to form tight sandstone and conventional reservoirs, hydrocarbons with good mobility can also remain in the laminae of the organic-rich layer (Jarvie, 2012; Han et al., 2015; Raji et al., 2015; Jubb et al., 2019; Hackley et al., 2020; Zhang et al., 2021; Hu et al., 2023, 2024).

Herein, a method ensuring that the resource data of various hydrocarbons (conventional, tight and shale) was developed that align with geological principles and provides constraints. It should be noted that expelled hydrocarbons may also form oil and gas accumulations such as asphalt or heavy oil, and conventional hydrocarbon reservoirs formed by the expelled hydrocarbons in the early stage may be transformed into tight oil and gas reservoirs through the burial and compaction, which are not discussed because they involve more complex geological processes. The Dongpu Depression in the Bohai Bay Basin has been well explored, generating ample geological and analytical test data. Diverse types of reservoirs have been identified in it, serving as a suitable area to apply this method. This study initially focuses on the identification of source rocks, leveraging hydrocarbon generation kinetics and Monte Carlo simulations to model a hydrocarbon evolution with changes in Ro, and use mass-conservation principles to identify and discuss microsource and microstorage shale. Effective hydrocarbon source rocks are defined as organic-rich rocks capable of expelling hydrocarbons, i.e., microsource shale. In addition, two formulas are developed to calibrate errors resulting from conventional sample handling and experimental pyrolysis processes. Based on effective source rock data, the HGE trends modeled and relative contribution of hydrocarbons generated from source rocks to different hydrocarbon reservoirs is discussed (Fig. 2c). This study allows for an evaluation of the theoretical maximum hydrocarbon resource potential associated with the hydrocarbon source rocks. By constraining the total hydrocarbon generation and expulsion through the use of migration and recovery factors, this provides a basis for predicting resources for different geological and extraction technology conditions.

2. Regional geological background

The northern Dongpu Depression was selected as the research area to demonstrate the effectiveness of the model. This area has experienced limited tectonic disruption and contains shale, tight, and conventional oil and gas resources, and also includes laminar shales and thin interlayer sandstones, which will make micromigration within the shale sequence more pronounced.

The Dongpu Depression is located on the southwestern edge of the Bohai Bay Basin, China, with a north–northeast orientation and an area of ~5300 km^2 (Fig. 3a and b). It is a Cenozoic salt-faulted lake basin with multiple sedimentary rhythms (Hu et al., 2022). The basin is characterized by multiple depressions and uplifts, including the Maxi Slope, Central Uplift, Liutun Depression, Haitongji Depression, Qianliyuan Depression, Pucheng Depression, and Lanliao Slope (Wang et al., 2015; Li et al., 2021). The Shahejie Formation (Es) in the northern salt-bearing area is the main exploration target in the Dongpu Depression, which can be divided into fourth (Es_4), third (Es_3), second (Es_2), and first (Es_1) members from bottom to top, fourth (Es_4), third (Es_3), second (Es_2), and first (Es_1) members from bottom to top. Above this strata is the Paleocene Dongying Formation (Ed), Neogene Guantao (Ng), Minghuazhen (Nm), and Quaternary Plain Formations (Py), with a maximum sedimentary thickness of >8000 m (Fig. 4). Overall, it mainly comprises gray shale, red shale, and siltstone, that formed as a result of high-frequency variations in depositional conditions (Zeng et al., 2013; Ji et al., 2018). Shale is commonly developed in the northern part of the depression during Es_3 and Es_4, which show numerous shale and thin sandstone layers, which are the main organic-rich rocks (Wang et al., 2015).

The early commercial petroleum flow in the Dongpu Depression mainly originated from the shallow conventional reservoirs of Es_3 and Es_1. However, in recent years, conventional oil and gas resources have faced depletion due to prolonged extraction. The enrichment of oil and gas indicates that deeper strata, including source rocks and adjacent

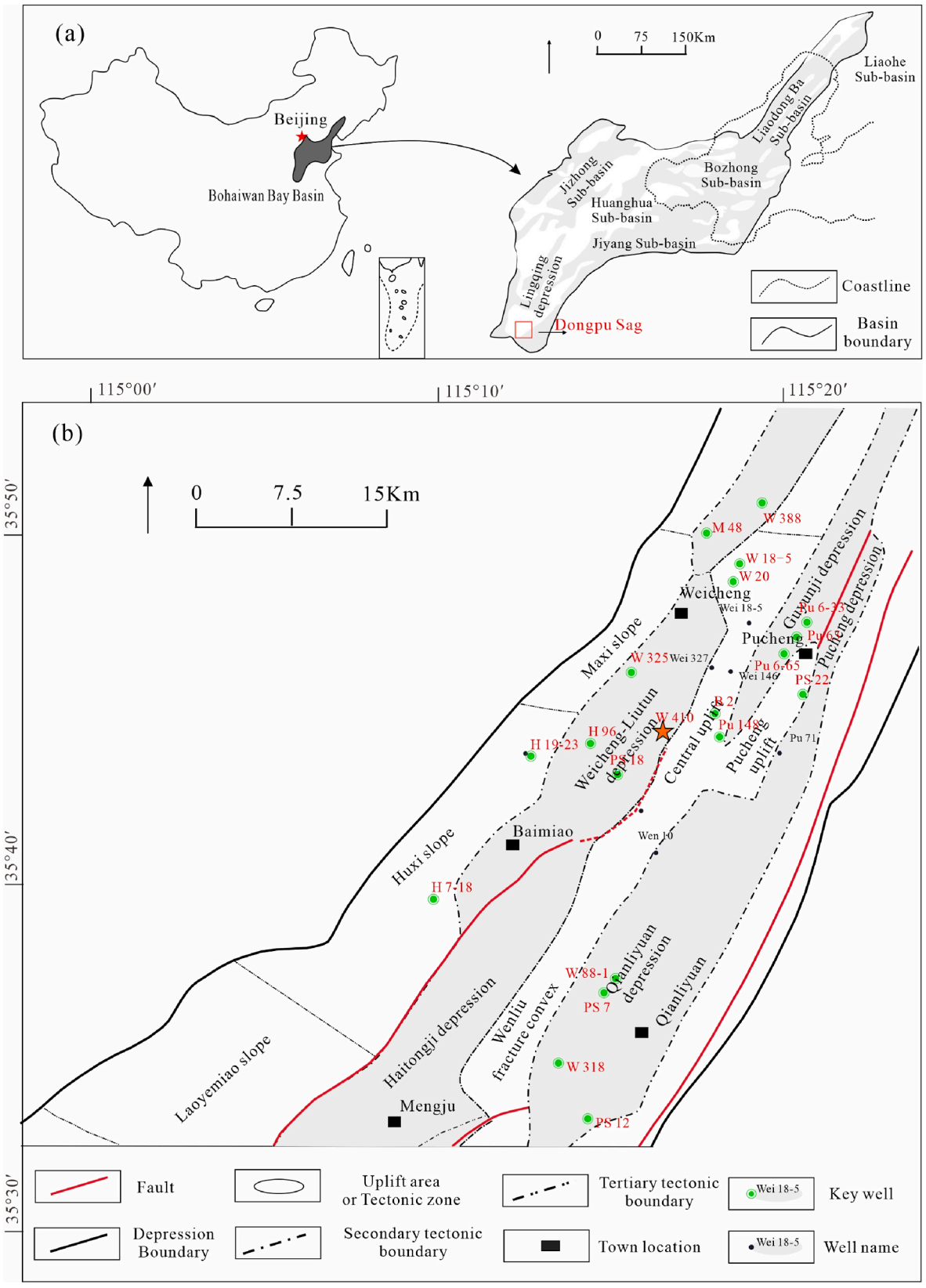

Fig. 3. Regional geological overview (modified from Wang et al., 2022; Hu et al., 2023). (a) Location of the Dongpu Depression in the Bohai Bay Basin, (b) planar and structural distribution of the Dongpu Depression.

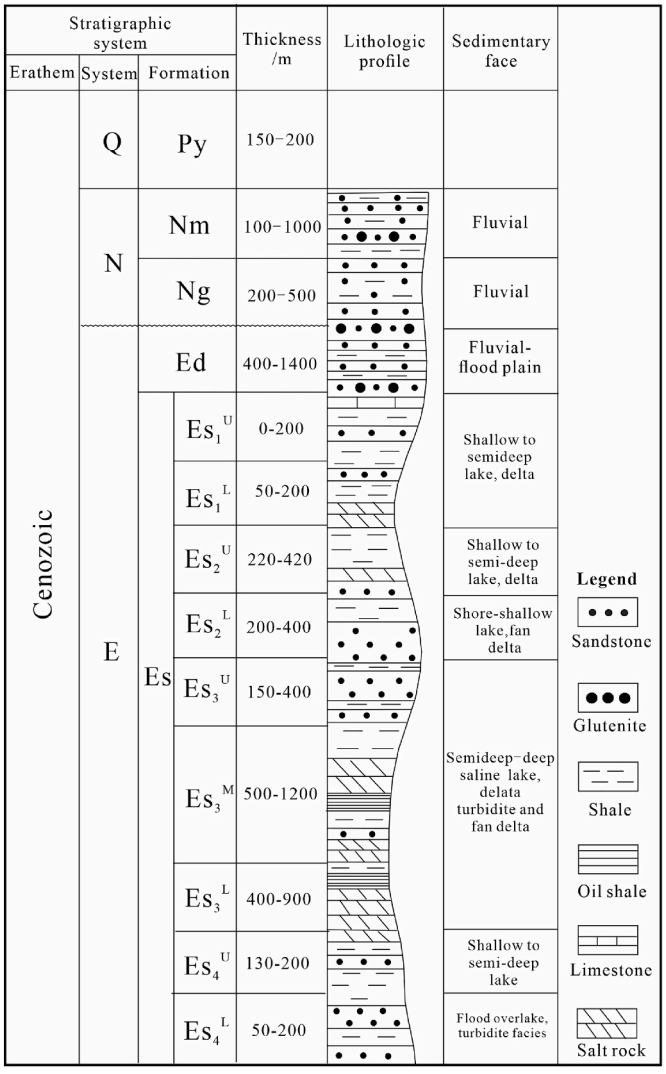

Fig. 4. Cenozoic stratigraphic column chart of the Dongpu Depression (modified from Hu et al., 2023).

tight reservoirs, may contain even more abundant oil and gas resources. Therefore, the focus of exploration is gradually shifting toward shale and tight sandstone reservoirs in the middle and lower parts of Es_3 (i.e., Es_3^M and Es_3^L, respectively) and upper parts of Es_4 (Es_4^U).

3. Material and methods

3.1. Databases

Data used herein were sourced from the Sinopec Zhongyuan Oilfield. In particular, 381 samples from 21 key wells were collected from the middle part of the third member of the Shahejie Formation in the northern Dongpu Depression. Sampling was distributed as much as possible in the plane to ensure that the model was representative. Notably, a series of experimental data for the same sample were obtained, including data on pyrolysis parameters, TOC, and Ro, and mineral composition.

3.1.1. Pyrolysis and total organic carbon

Pyrolysis data were obtained according to the National Standard of the People's Republic of China: Rock pyrolysis analysis (GB/T 18602-2012) drafted by Wu et al. (2012). Samples are first crushed to a particle size of 0.15 mm or less, and were tested in an OGE-II pyrolysis instrument. Each sample was subjected to a temperature of 300 °C and the S1 hydrocarbon peak (mg/g of rock) was quantified. Then, programmed pyrolysis was performed with temperatures increasing from 300 °C to 650 °C to quantify the potential hydrocarbons (peak S2, mg/g of rock). The temperature corresponding to the maximum hydrocarbon yields is termed Tmax.

TOC data were obtained according to the National Standard of the People's Republic of China: Determination of total organic carbon in sedimentary rock (GB/T 19145-2003) drafted by Xu et al. (2003). Before the experiment, samples were weighed (about 1g) and ground to a diameter less than 0.2 mm. Then, inorganic carbon was removed by dilute hydrochloric acid (HCl: H_2O = 1:7), and samples were tested in an LECO CS-744 carbon sulfur instrument.

3.1.2. Vitrinite reflectance

Vitrinite reflectance (Ro) data were obtained according to the oil and gas industry standard of the People's Republic of China: Method of determining microscopically the reflectance of vitrinite in sedimentary (SY/T 5124-2012) drafted by Tu et al. (2012). Samples were examined using a LEICA DM 4P instrument. Due to the small differences in optical properties between particles in the same sample, it is important to take a sufficient number of reflectance measurements from different particles to ensure that the results are representative. Generally, the number of measurement points should be greater than 20 (Barker and Pawlewicz, 1993).

3.1.3. Other analytical tests

For accurate quantitative analysis, the samples were obtained from well W410, a shale-dedicated exploration well. 225 rock samples were collected from its shale layers, with sampling conducted at an interval of 3 samples per meter. Multistep pyrolysis (GB/T 18602-2012), freeze–thaw pyrolysis (GB/T 18602-2012) was conducted, and whole-rock mineral X-ray diffraction experiments were also performed.

Multistep pyrolysis and freeze–thaw pyrolysis follow the same Chinese standards as conventional pyrolysis. However, in the specific experimental procedure they have some differences from conventional pyrolysis. For freeze–thaw pyrolysis, freshly extracted rock samples were either cryopreserved at low-temperature (−60 °C) in the laboratory for 24h or immediately underwent cryogenic pyrolysis experiments. In the experiments, an automatic cryogenic grinder (Cryomill) and a pyrolysis instrument (HAWK) provided by the Sinopec Wuxi Research Institute of Petroleum Geology was used to ensure that the samples remained at liquid-nitrogen temperature (−196 °C) throughout the crushing process. For multistep pyrolysis, each sample was subjected to a temperature of 200 °C and free hydrocarbons (peak S1-1, mg/g of rock) was quantified. Then, programmed pyrolysis was performed with temperatures increasing from 200 °C to 350 °C to quantify the medium-heavy components of free hydrocarbons (peak S1-2, mg/g of rock). Subsequently, another programmed pyrolysis was performed with temperatures increasing from 350 °C to 450 °C to quantified the bound hydrocarbons (peak S2-1, mg/g of rock). Last, programmed pyrolysis was performed with temperatures increasing from 450 °C to 600 °C to quantified the potential hydrocarbons (peak S2-2, mg/g of rock) (Jiang et al., 2016).

Mineral composition data were obtained according to the oil and gas industry standard of the People's Republic of China: Analysis method for clay minerals and ordinary non-clay mineralsin sedimentary rocks by the X-ray diffraction (SY/T 5163-2018) drafted by Zeng et al. (2018). Samples was first oil washed and subsequently crushed to a particle size of less than 40 μm. Then, samples were examined using diffractometer (Ultima-IV X-ray diffractometer instrument) at conditions of 20 mA and 40 kV with a curved graphite monochromator. Finally, the obtained X-ray diffraction spectra were used to identify and quantify various types of minerals.

3.2. Workflow

The steps involved in constructing an resource evaluation model are shown in Fig. 5, including (1) data of collection; (2) calibration of light and adsorbed hydrocarbons; (3) restoration of the original hydrocarbon generation potential to identify the results of hydrocarbon micro-migration; (4) calibration of microsource and microstorage shale to determine if the shale is effective; and (5) establishment of the HGE model to calculate the amount of hydrocarbons generated, expelled, and trapped the source rock. The HGE model was based on source rocks capable of effectively expelling hydrocarbons. Therefore, samples with extremely low S1, S2, and TOC values were excluded to ensure accuracy of the HGE pathway.

3.2.1. Calibration of light and heavy hydrocarbons

Conventional pyrolysis has certain limitations, which are reflected in two aspects: first, the inevitable loss of light hydrocarbons during sample collection and storage leads to lower S1 contents. Second, there may be difficulty in effectively distinguishing between S1 and S2 because some generated heavy adsorbed hydrocarbons can be incorporated into the S2 peak(Clementz, 1979; Delvaux et al., 1990; Jarvie, 2012). The actual S1 content of crude oil in a shale ($S1_0$) should include the measured S1 content, light hydrocarbon lost before pyrolysis analysis ($S1_C$), and heavy residual hydrocarbons detected as S2 ($S2_C$). Before model establishment, compensation calibration for light and heavy hydrocarbons should be performed. In this study, a simple calibration model for light and heavy hydrocarbons was developed based on multistep and freeze–thaw pyrolysis analysis.

During sampling while drilling, the phase equilibrium of hydrocarbons in the sample changes from the state under reservoir temperature and pressure conditions to that of surface conditions, and with oil dropping out of the gas phase (Chen et al., 2019). After sampling, the gas remaining in the sample as well as a portion of the light hydrocarbon fraction is likely to be lost during sample preservation and sample crushing (Jarvie, 2014). Although it was not possible to calibrate for the loss of light hydrocarbons during sampling, the loss of hydrocarbons after sampling is fully avoided by freeze–thaw pyrolysis. Through conventional and freeze–thaw pyrolysis of the samples to obtain the original $S1_C$ content and conventional S1 content, the relationship between the original $S1_C$ contents and TOC values and the conventional S1 contents using the multivariate fitting function of SPSS software was established, as shown in Equation (1). The predicted values correlated well with the experimental values (Fig. 6a).

$$S1_C = 0.133 \times TOC + 1.143 \times S1 + 0.134 \quad (1)$$

Multistep rock pyrolysis is an improved method used to determine the free hydrocarbon content (S1-1), pertaining to the light component of free hydrocarbon present in the connected pores of shale. Further, S1-2 represents the content of medium-heavy components of free hydrocarbon, S2-1 represents the content of bound hydrocarbons, and S2-2 represents the content of potential hydrocarbons (Clementz, 1979; Delvaux et al., 1990; Jarvie, 2012). Conventional and multistep

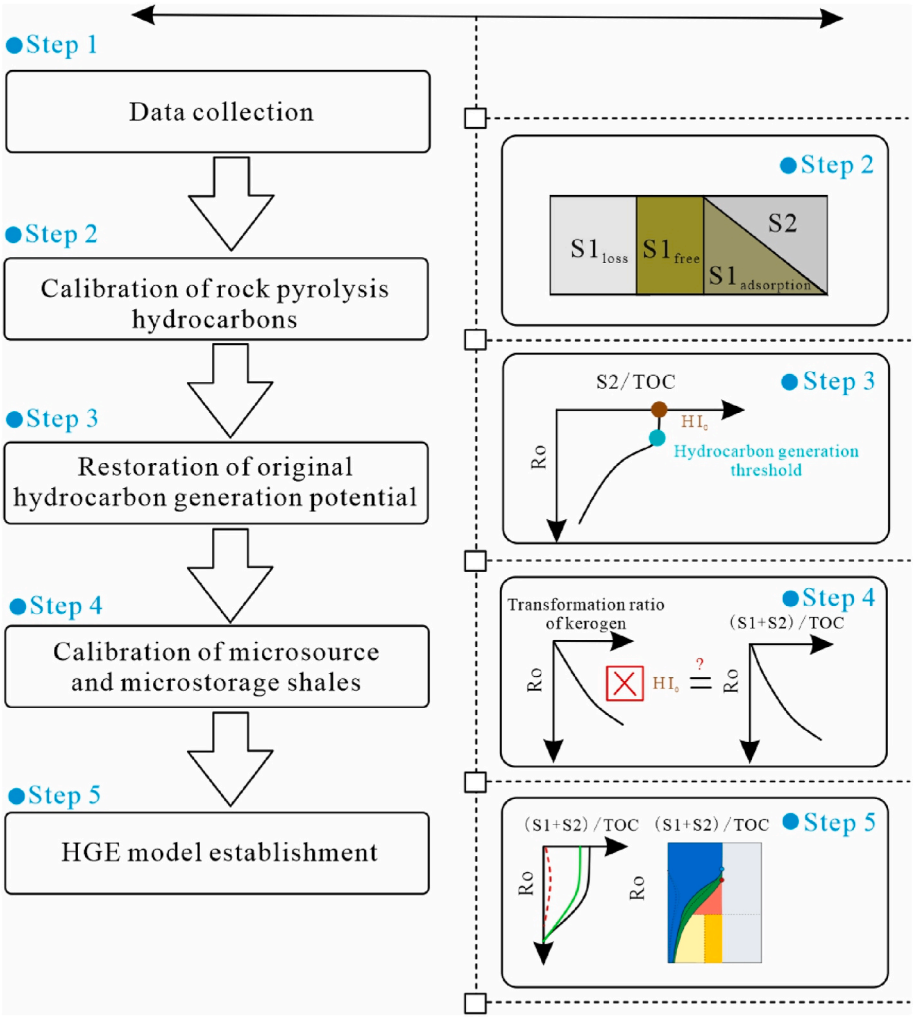

Fig. 5. Workflow of the proposed method.

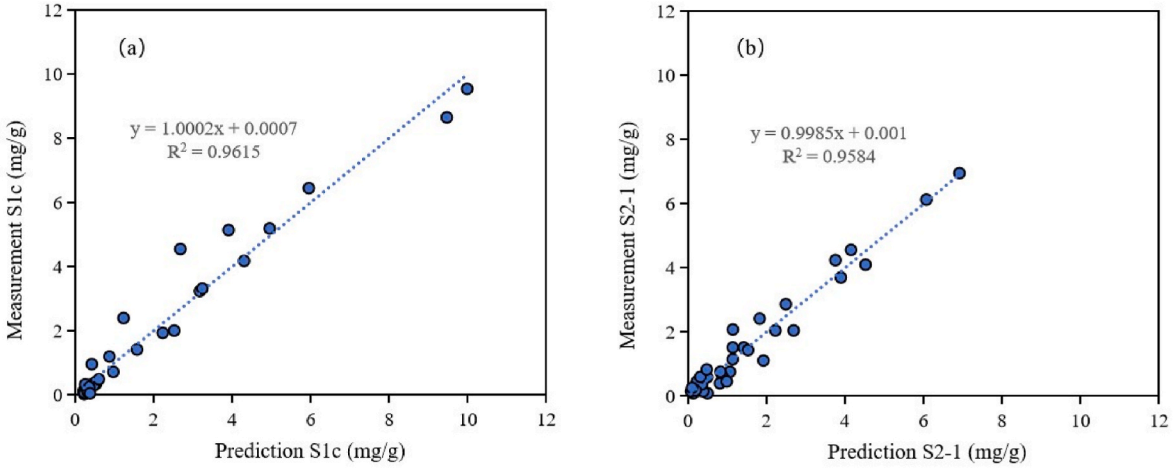

Fig. 6. Correction of predicted light and heavy hydrocarbons.

pyrolysis analyses were performed for the samples and the relationship between $S2_C$ (content of bound hydrocarbons) and TOC values and conventional S2 contents was established as before, as shown in Equation (2); the predicted values showed good correlation with experimental values (Fig. 6b):

$$S2_C = 0.102 \times S2 + 0.692 \times TOC - 0.359 \quad (2)$$

3.2.2. Restoration of the original hydrocarbon generation potential

After HGE, the hydrocarbon content of rocks can be significantly reduced. Before model establishment, the original hydrocarbon generation potential should be restored. Li et al. (2020) introduced a hydrocarbon generation kinetics calculation formula (Equation (3)) for the original hydrogen index (HI_0 = S2/TOC) and original hydrocarbon generation potential index (GPI_0 = (S1 + S2)/TOC). First, identify the kerogen type of the hydrocarbon source rock by HI-Tmax cross-plots and roughly estimate the distribution of the original hydrocarbon potential (HI_0) of the immature hydrocarbon source rock. Secondly, the evolutionary plots of HI for all samples under different maturity levels are established. Finally, Monte Carlo simulation is used to obtain the parameters in Eq. (3) under the optimal evolutionary path. In this study, because S1 was not generated in the immature organic-rich rocks, HI_0 and GPI_0 were equal. Hence,

$$HI\,(Ro) = \frac{\mathrm{HI}_0}{\left(1 + e^{\left(\theta 1 \times \ln\left(\frac{Ro}{\beta 1}\right)\right)}\right)} \quad (3)$$

where HI denotes the hydrogen index (mg HC/g TOC), Ro denotes the vitrinite reflectance (%), HI_0 denotes the original hydrogen index (mg HC/g TOC), β1 is a dimensionless parameter and reflects Ro corresponding to a large amount of hydrocarbon generation, and θ1 is a dimensionless parameter and reflects the Ro range of hydrocarbon generation.

On this basis, the plot of HI transformation rate (HI_{TR}) versus Ro was fitted, and the HI_{TR} value of each sample was obtained from Ro as follows:

$$HI_{TR}\,(Ro) = \frac{1}{\left(1 + e^{\left(\theta 1 \times \ln\left(\frac{Ro}{\beta 1}\right)\right)}\right)} \quad (4)$$

3.2.3. Calibration of microsource and microstorage samples

For the convenience of description, three types of reservoirs are defined. The first being shale that act as hydrocarbon source rocks, which are themselves tight and generate large quantities of hydrocarbons that are trapped in situ. The first category can be divided into two sub-types: organic-rich shale reservoirs with hydrocarbons trapped in situ, and mixed shale with organic-poor interlayers. The second category is the tight reservoir excluding shale, which includes tight sandstone and tight carbonate rock, positioned near the hydrocarbon source rock. The third category is conventional reservoirs, which have relatively good reservoir properties and are usually away from the hydrocarbon source rocks (Fig. 7). Organic-rich shale reservoirs is difficult to extract without enhancement, it can be considered as a potential resource. Meanwhile, mixed shale and tight reservoirs have become the main unconventional petroleum products, which are referred to as favorable domains for petroleum exploration (Jarvie, 2012; Hu et al., 2018).

Using HI and HI_{TR}, the theoretical GPI_0 value of each sample under different degrees of thermal alteration can be calculated and compared with the calibrated measured hydrocarbon generation potential GPI_1. The source and reservoir discrimination coefficient (ΔQ) is introduced, which represents the relative intensity of the hydrocarbon generation and storage capacity, because this parameter also represents whether the shale is expelling or receiving hydrocarbons (Hu et al., 2023, 2024):

$$\Delta Q = \mathrm{GPI}_0 - \mathrm{GPI}_1 \quad (5)$$

Notably, $\Delta Q > 0$ indicates that the sample is a shale that has undergone hydrocarbon expulsion, while $\Delta Q < 0$ indicates that the sample is a shale that accepts external hydrocarbons. Storage shale suggests that the storage properties of this sample are relatively good compared to other samples, where the organic-poor lamina or tight interlayer receives the expelled hydrocarbons from the other shale samples. Previous studies have shown that such micromigration occurs due to differences in hydrocarbon expulsion, pore space, and capillary pressure among shales (Hu et al., 2023). In addition, the reliability of the micromigration evaluation results were verified by combining the group components based on the geochromatography effect, two-dimension nuclear magnetic resonance analysis, and the geochemical behavior of inorganic elements such as manganese during the process of hydrocarbon migration (Hu et al., 2024). On this basis, samples that served as microstorage shale (i.e., $\Delta Q < 0$) were removed. Generally, there are Type II outside shale systems. Meanwhile, continuous shale systems often have partially tight layers (sandstone and limestone, etc.) inside, because of their extremely weak hydrocarbon generation potential, they are all considered as tight reservoirs (Fig. 7). After dividing the microsource and the microstorage shale, ΔQ and TOC values were used to calculate the proportion of hydrocarbons received in various reservoirs in total expelled hydrocarbons in the organic-rich layer.

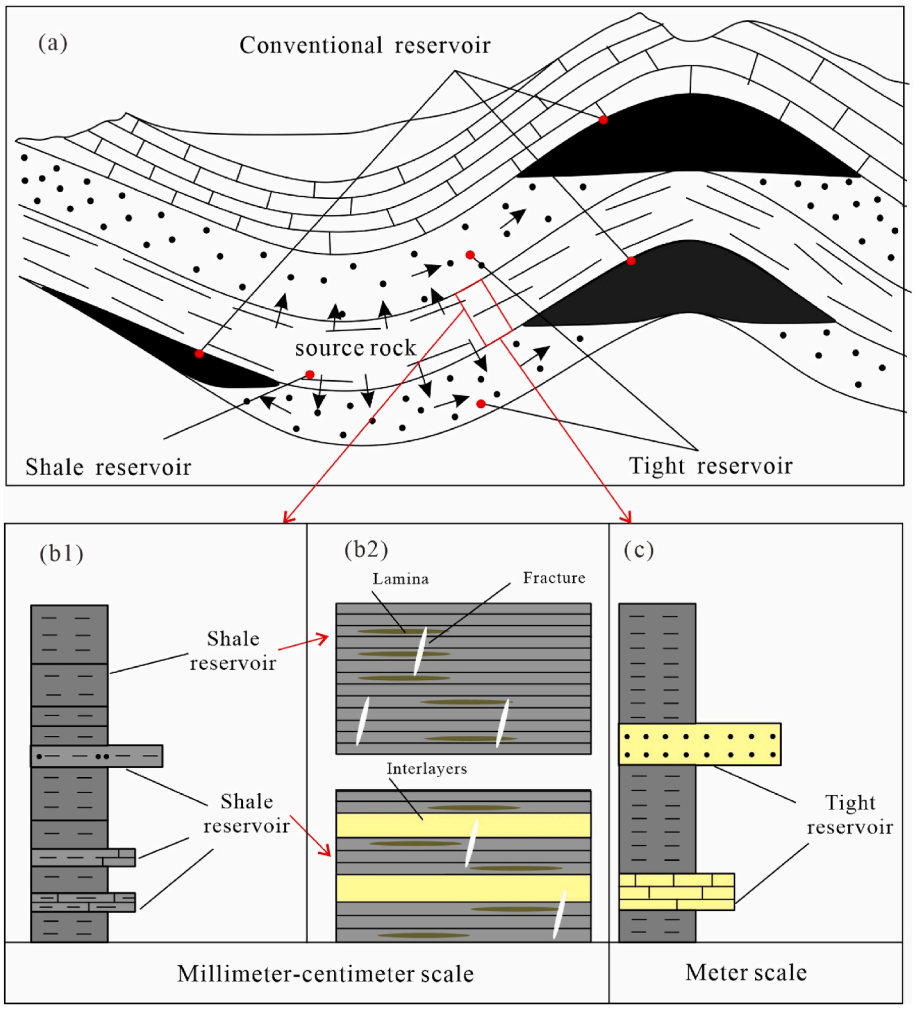

Fig. 7. Schematic of the reservoirs (modified from Tissot and Espitalié, 1975). (a) Distribution of conventional, tight and shale reservoirs. (b) Shale lamina and interlayer reservoirs at millimeter and centimeter scales. (c) Tight reservoirs in shale formations at the mid-meter scale.

3.2.4. HGE model establishment

The principle of conservation of mass requires that the total mass of hydrocarbons which come from source rock remains unchanged before and after HGE. Therefore, the amount of hydrocarbons generated before expulsion equals the amount of retained hydrocarbon. After expulsion the total hydrocarbons represent equals the sum of the amounts of retained hydrocarbon and expelled hydrocarbon. The total organic matter in rocks is categorized as: (1) residual organic matter, which has not yet been converted into hydrocarbons and can be represented by the HI; (2) hydrocarbons generated and retained, represented by the hydrocarbon index HCI (S1/TOC); and (3) hydrocarbons expelled. The HGE characteristics of organic-rich rocks were analyzed through variations in the GPI on the rock profiles. GPI characterizes the total hydrocarbon generation potential per unit TOC, considering generated residual free hydrocarbons and unconverted pyrolysis hydrocarbons (Pang et al., 2005).

Three critical boundary conditions required are clarified in the following. The first geochemical boundary is the hydrocarbon expulsion threshold (HET), which corresponds to a significant GPI reduction due to hydrocarbon expulsion (Pang et al., 2005). The second boundary is termed the hydrocarbon generation threshold (HGT), which corresponds to the significant HI reduction and TR increase due to hydrocarbon generation (Tissot and Espitalié, 1975). The third boundary is termed the buoyancy-driven hydrocarbon accumulation depth (BHAD), which corresponds to the where the reservoir becomes tight due to constant compaction at increasing depths of burial. After the reservoir is tight, the capillary resistance is significantly greater than the buoyancy force, and the hydrocarbons can only be driven by non-buoyancy forces in the reservoir. At the same time, the boundary also implies that the hydrocarbons expelled from the neighboring hydrocarbon source rocks transform from conventional reservoir aggregation to the tight reservoir accumulation (Pang et al., 2021).

First, assuming that HI_0 is equal to GPI_0 the functional relationship between GPI and Ro is determined using the same method as HI_0. Subsequently, the functional relationship between HCI and Ro was obtained based on the fact that GPI = HI + HCI. Then, the hydrocarbon TR and expulsion rate (ER) were calculated (Equations (6)–(11)) (Li et al., 2020). Based on this, the evolution process of HGE from organic-rich rocks was established. Finally, the restoration of the original rock quality (G_0) and original TOC (TOC_0) of organic-rich rocks provided parameters for resource potential assessment.

$$GPI\,(Ro) = \frac{\mathrm{GPI_0}}{\left(1 + e^{\left(\theta 2 \times \ln\left(\frac{Ro}{\beta 2}\right)\right)}\right)} \tag{6}$$

$$HCI\,(Ro) = GPI\,(Ro) - HI\,(Ro) \tag{7}$$

$$TR = \frac{\mathrm{HI_0} \times (1000\mathrm{a} - HCI) - 1000\mathrm{a} \times HI}{\mathrm{HI_0} \times (1000\mathrm{a} - HI - HCI)} \tag{8}$$

$$ER = \frac{1000a \times (GPI_0 - GPI)}{GPI_0 \times (1000a - GPI)} \quad (9)$$

$$TOC_0 = \frac{TOC}{1 - \frac{GPI_0}{1000a} \times ER \times \left(1 - a \times \frac{TOC}{100}\right)} \quad (10)$$

$$\varnothing = \frac{1}{\left(1 - \frac{GPI_0}{1000} \times \frac{TOC_0}{100} \times ER\right)} \quad (11)$$

where β2 denotes maturity corresponding to a large amount of hydrocarbon expulsion and θ2 denotes the range of hydrocarbon expulsion windows. α denotes the organic carbon hydrocarbon generation ratio (g HC/g TOC). The rock quality recovery coefficient φ (dimensionless) is defined as the ratio of the original rock mass (Go) to remaining rock mass (G), and TOC_0 is the original organic matter abundance (%).

Finally, the hydrocarbon generation efficiency and hydrocarbon expulsion efficiency is calculated for each period as required. On this basis, the hydrocarbon expulsion and generation rate efficiency, the hydrocarbon generation intensity, hydrocarbon expulsion intensity, hydrocarbon residual intensity, hydrocarbon generation quantity, hydrocarbon expulsion quantity, and residual-hydrocarbon quantity were determined. The related calculation formulas can be found in (Li et al., 2020) (Equations A1–A9).

4. Results

4.1. Geochemical characteristics

Based on pyrolysis data and classification criteria for lacustrine organic-rich rocks, the quality of Es_3^M shales was evaluated. The TOC values and S1 + S2 contents were in the ranges of 0.15 %–7.67 % (average = 1.26 %) and 0.21–46.75 mg HC/g rock (average = 5.41), respectively. HI values were in the range of 22.19–647.36 mg HC/g TOC (average = 181.31 mg HC/g TOC). The shales heterogeneity was high, with most samples representing fair to good shales (Fig. 8a). The type of kerogen can be determined using pyrolysis parameters. The Es_3^M shales in the Dongpu Depression mainly comprised Types II_1 and II_2 kerogen (Fig. 8b), and this is consistent with the results of previous analyses (Zhu et al., 2021).

Tmax and Ro are the most commonly used parameters for evaluating thermal maturity. The Tmax range of Es_3^M shales was 410°C–467 °C and mainly concentrated in the 430°C–450 °C range. Considering the effect of S2 content on Tmax (Katz and Lin, 2021), the Tmax for samples with S2 values greater than 1 ranges from 411°C to 450 °C and mainly concentrated in the 430°C–450 °C range, which means that most of the sample is already into the oil-window. The range of Ro was 0.27 %–1.65 % and mainly concentrated in the 0.5 %–1.2 % range, corresponding to low-to maturity stages (Fig. 7c).

4.2. Characteristics of hydrocarbon micromigration

4.2.1. Identification of micromigration

Micromigration is defined as the migration of hydrocarbons between lamina or thin interlayer layers within a shale sequence that have different hydrocarbon generation and storage capacities, as a response to differential hydrocarbon enrichment in the context of micro-source-reservoir structures within the shale sequence (Hu et al., 2024). Significant micromigration phenomena were observed in Es_3^M. When a source rock is immature, the PI (S1/(S1 + S2)) value should approach 0, while S2/(S1 + S2) should approach 1. Contamination by migrating hydrocarbons can alter these values (Han et al., 2015; Jiang et al., 2015; Li et al., 2018). Fig. 8a shows that for Tmax <430 °C, large PI values are observed, indicating a high S1 content. When Tmax = 430°C–450 °C, organic matter is still in the oil-window, previous studies have shown that the TR of organic matter are between 10 % and 60 % (Wu et al., 2024). As shown in Fig. 9a, many samples have PI values exceeding 60 %, and the oil saturation index (OSI: S1/TOC) value of most samples increases significantly with decreasing Tmax, inconsistent with the thermal alteration patterns of organic matter. In addition, the OSI of samples with high PI values was generally greater than 100 (bubble size represents the OSI value), which also implies that a significant oil across over effect may have occurred (Jarvie, 2012). Fig. 9b shows that the S2/(S1 + S2) value of shale exhibits the opposite trend, indicating that the samples maybe are storage shales that accepts external hydrocarbons.

Further, during the sedimentation of Es high-frequency climate variations resulted in varying stratigraphic depositional conditions, tight layers and shale layers are frequently interbedded macroscopically. At the microscopic level, there are tight organic-rich lamina that interact with felsic and carbonate organic-poor lamina. At the macroscopic level, the samples receiving migrating hydrocarbons have lower main peak carbon numbers in the saturated hydrocarbon total ion chromatogram of shale, higher ratios of saturated to aromatic hydrocarbons (Han et al., 2015; Patidar and Singh, 2024), and high TOC content, with sand interlayers or well-developed organic-poor lamina (Zeng et al., 2013) (Fig. 10a). The main peak carbon number of the total ion chromatogram in the expelled from the hydrocarbon section is relatively large, generally comprising shale blocks or highly developed organic-rich lamina (Fig. 10b).

Microscopically, as observed in the fluorescence images of laser confocal scanning, there is a higher content of heavy components in the organic-rich interlayers. The content of light components in organic-poor lamina is significantly higher than that of heavy components, which mostly develop with a long strip-like bedding pattern. These

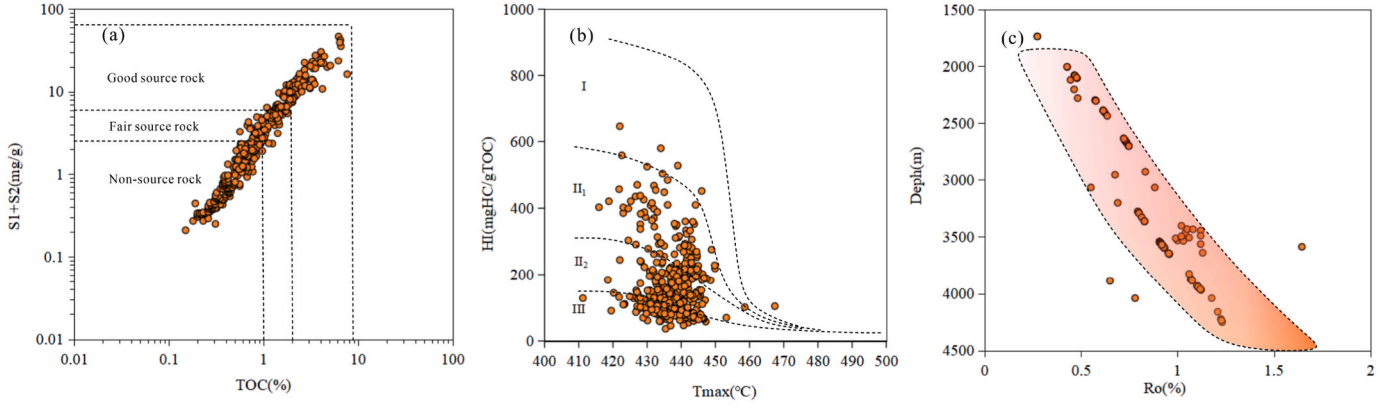

Fig. 8. Geochemical characteristics of shales in Es_3^M. (a) organic matter abundance, (b) kerogen type, and (c) maturity.

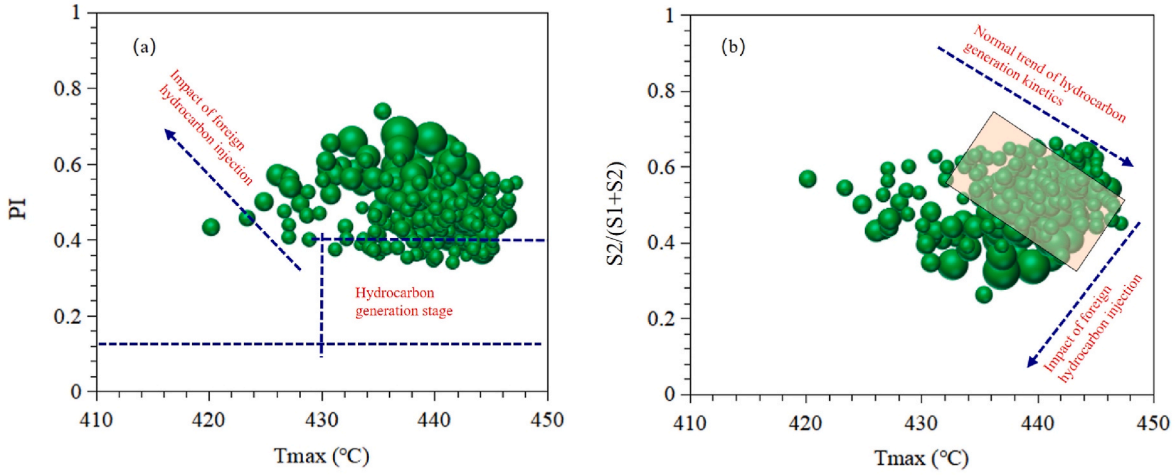

Fig. 9. Hydrocarbon micromigration diagram. (a) Intersection diagram of Tmax and PI, where the size of the green bubbles represents the OSI value. (b) Intersection diagram of Tmax and S2/(S1 + S2), where the size of the green bubbles represents the OSI value. (For interpretation of the references to colour in this figure legend, the reader is referred to the Web version of this article.)

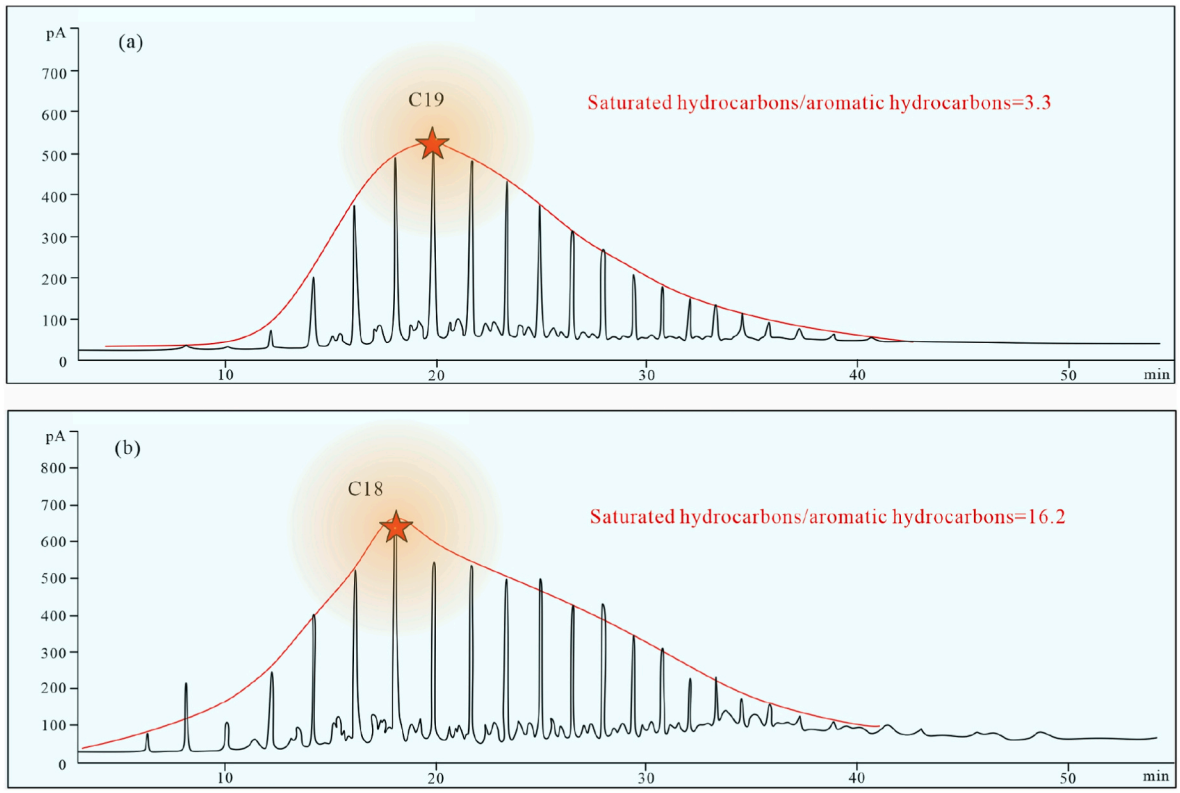

Fig. 10. Saturated hydrocarbon total ion chromatogram of shale. (a) W408 (4560.6 m, ΔQ: 70.45 mg/g, TOC: 1.16 %). (b) W408 (4563.5 m, ΔQ: −27.13 mg/g, TOC: 0.69 %).

results indicate significant micromigration (Gao et al., 2023). Microscopic hydrocarbon components can be used to determine whether shale sample is hydrocarbon-expelling or hydrocarbon-receiving, with organic-rich minerals (laminae) typically expelling hydrocarbons with a heavier heavy component, while organic-poor minerals (laminae) typically receiving hydrocarbons with a lighter component. The TOC and mineral composition (laminae structure) of shales significantly affects hydrocarbon micromigration because hydrocarbon migration may need to be driven by the overpressure generated by hydrocarbon generation, and laminae seams may be good pathways for migration. There were four hydrocarbon migration modes observed: (1) low-abundance shale (TOC = 0.25 %, ΔQ = 11.19 mg/g) releases a small amount of hydrocarbons outward (Fig. 11a). At this time, some heavy hydrocarbons are retained in the shale, and the hydrocarbon content depends on the hydrocarbon generation potential of the shale and the amount of hydrocarbons expelled; (2) low-abundance shale (TOC = 0.11 %,ΔQ = −126.42 mg/g) stores some of the expelled light hydrocarbons from other shale. Generally, because of low amount of organic-poor minerals, the content of foreign hydrocarbons is poor (Fig. 11b); (3) mixed rocks (TOC = 2.04 %,ΔQ = 190.68 mg/g) contain organic-poor blocks or lamina, and lots of laminated seam along with high-abundance. Generally, because of the lack of organic-poor layers or fewer pores,

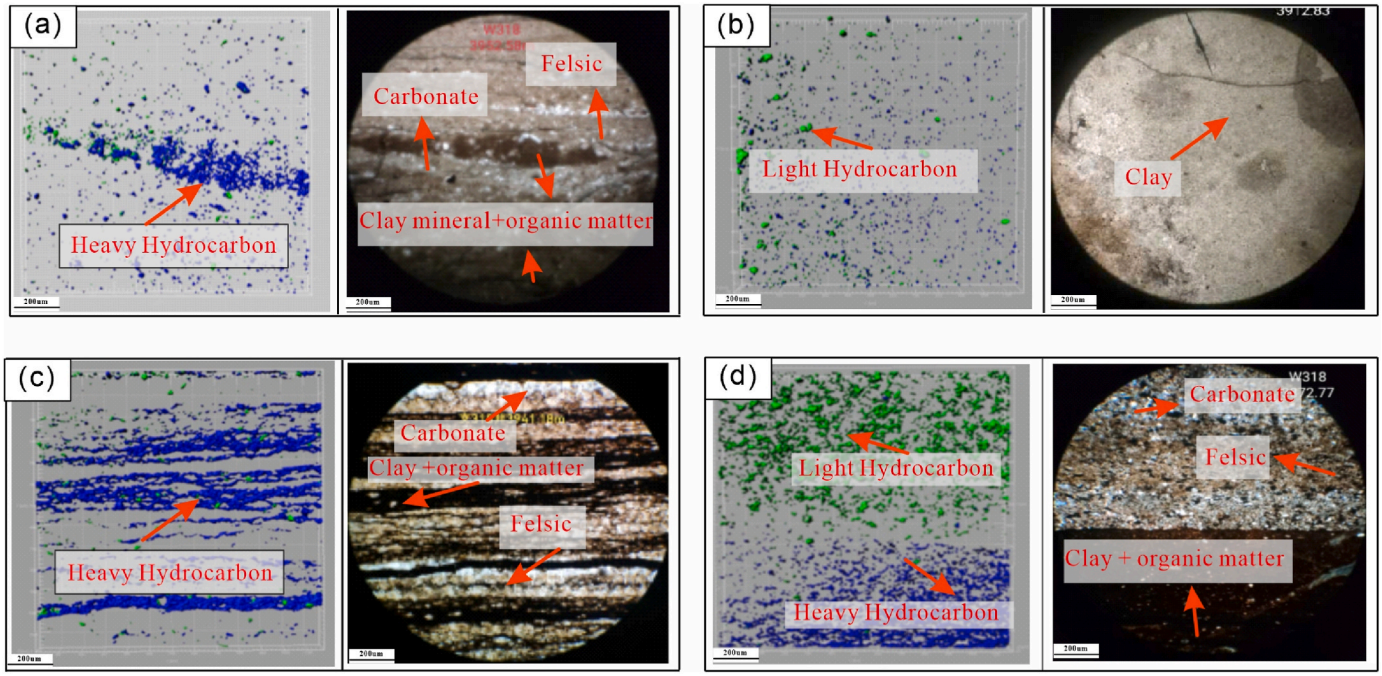

Fig. 11. Laser confocal scanning image. (a) Shale (ΔQ: 11.19 mg/g, TOC: 0.25 %; oil content: 1.86 %): low HGE ability. (b) Shale (ΔQ: −126.42 mg/g, TOC: 0.11 %; oil content: 0.93 %): low hydrocarbon generation ability and reception of hydrocarbons. (c) Mixed shale (ΔQ: 190.68 mg/g, TOC: 2.04 %; oil content: 6.21 %): low hydrocarbon storage and expulsion ability. (d) Mixed shale (ΔQ: −91.39 mg/g, TOC: 1.08 %; oil content: 2.19 %): high hydrocarbon storage and reception ability.

hydrocarbon expulsion occurs and the oil content is good (Fig. 11c); and (4) mixed rocks (TOC = 1.08 %,ΔQ = −90.39 mg/g) contain organic-poor blocks or lamina, but their abundance is medium. Generally, because of the abundance of organic-poor lamina or the development of pores, they mainly receive hydrocarbons and their oil-bearing properties are good (Fig. 11d).

4.2.2. Micromigration evaluation

A model for the evolution of HI and HI_{TR} with respect to Ro was developed for shale samples obtained from Es_3^M (Fig. 12); the blue line represents the best fit, and the black line represents 10,000 Monte Carlo simulation paths indicating the uncertainty of the predicted variables. Theoretically, HI_0 and GPI_0 are equivalent when organic-rich rocks are immature. However, in actual geologic conditions, there is usually a small amount of S1 present. The values between HI and GPI were compared under low-maturity conditions (Ro < 0.5 %) and found a 6 % difference. Based on this, when ΔQ < 6 % for original hydrocarbons, it is believed that hydrocarbon expulsion and reception have not occurred.

The results of the hydrocarbon micromigration evaluation revealed that ΔQ ranged from −300 to 360 mg/g, concentrating mainly between −100 and 100 mg/g, with an average of 27.41 mg/g. Particularly, 26 % of microstorage shales received hydrocarbons and 62 % of microsource shales expelled hydrocarbons. The intersection diagram of ΔQ and OSI showed good mobility of the hydrocarbon microstorage shales, attributable to S1 migration. Thus, samples with lesser expulsion exhibited higher mobility (Fig. 13a). The intersection plot of ΔQ and S1+S2 showed that the microstorage and microsource samples had high S1+S2. When the absolute value of ΔQ increased, the S1+S2 increased (Fig. 13b). This is because microstorage shales receive a large amount of transported S1 and microsource shales often have a greater hydrocarbon generation ability, indicating that layers with good organic-rich quality are mainly characterized by hydrocarbon expulsion; however, this does

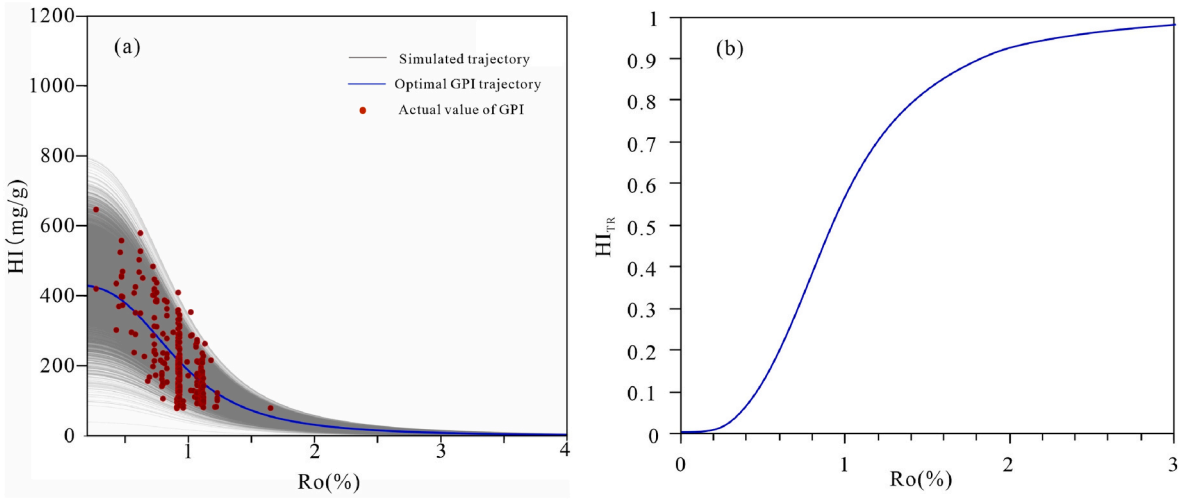

Fig. 12. Evolution path and HI_{TR} model of HI. (a) Evolution path and HI and (b) evolution path and HI_{TR}.

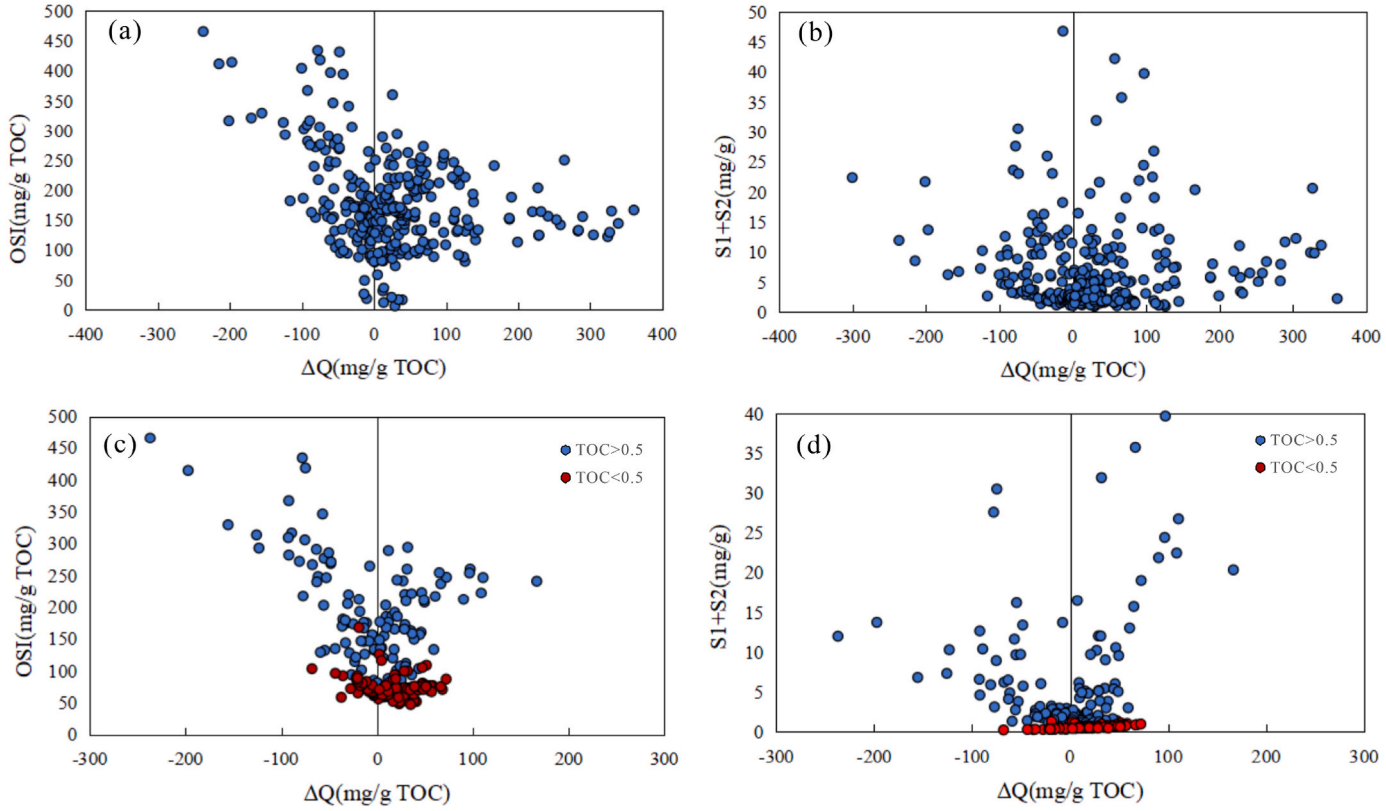

Fig. 13. Micromigration hydrocarbon quantity evaluation chart. (a) ΔQ and OSI of all wells. (b) ΔQ and (S1 + S2) of all wells. (c) ΔQ and OSI of W410. (d) ΔQ and (S1 + S2) of W410.

not mean that their hydrocarbon content is poor. The accumulated hydrocarbon generated by the source is still substantial. This trend is closely related to the ER of organic-rich rocks, which is controlled by thermal maturity, physical properties, microstructure, and minerals composition of the shale.

The hydrocarbon micromigration evaluation results of 225 samples from W410 continuous sampling showed similar characteristics. For samples with low TOC values, the mobility decreased and S1+S2 increased with increasing ΔQ, confirming the aforementioned viewpoint (Fig. 12c and d). In particular, 64 samples are microstorage, accounting for 28.4 % of the total samples, with an average hydrocarbon concentration of 51 mg/g (TOC content = 1.09 %). The average hydrocarbon reception of felsic and carbonate shale was 92 mg/g (TOC content = 2.09 %), accounting for ~6.6 % of the total samples. Clay shale receives an average of 36 mg/g of hydrocarbons (TOC content = 0.73 %), accounting for ~21.8 % of the total samples. Shale with more organic-poor minerals and high TOC receive more hydrocarbons, probably because only shale with enough organic matter to generate pressure of the fluid can drive the migration of hydrocarbons. This also implies that hydrocarbon micromigration usually occurs where there is high TOC and good reservoir performance, which may be within shale with high organic matter abundance and high organic-poor mineral content, or shale with high TOC may migrate to adjacent tight sandstone reservoirs, but it is difficult to break through the capillary resistance for long-distance migration in shale. The number of microsource samples is 135, accounting for 71.6 % of the total samples. The average amount of expelled hydrocarbons is 33 mg/g (TOC content = 1.0 %). Meanwhile, 33.2 %, and 25.7 % of the internal hydrocarbon expulsion are received by the clay shale and felsic (or carbonate) shale, respectively, indicating that up to 41.1 % of expelled hydrocarbons enter tight and conventional traps outside shales.

4.3. HGE model

Based on the micromigration evaluation results, the microstorage shales were excluded. Next, an HGE model for Es_3^M shales was established (Fig. 14a). Herein, α was set to 1.2 (Burnham, 1989). The main samples in the study area were Type II kerogen, and the model revealed that HGT and HET were 0.37 % and 0.68 % Ro, respectively, with an GPI_0 of 490 mg/g HC. Once HGT and HET were reached, the TR and ER first increased rapidly and then slowly, with an average value of about 60 % (Fig. 14b). With increasing thermal maturity, the efficiency of HGE first increased rapidly and then slowly. The peak hydrocarbon expulsion and generation rates of Es_3^M shales were 0.8 % and 1.2 % Ro, respectively, with corresponding maximum rates reaching 475 and 468 mg/g/0.1 % Ro (Fig. 14c).

5. Discussion

5.1. Effect of geochemical characteristics on HGE potential

In this study, multistep and freeze–thaw pyrolysis analyses were performed for error correction of light and heavy hydrocarbons. Using well W410 as an example, the original average S1 and S2 contents of samples were determined to be 0.92 and 2.63 mg/g, respectively, while the corrected S1 and S2 contents were 1.95 and 2.00 mg/g, respectively. The loss of S1 reached 53 %, and S2 increased by 32 % of the original. When pyrolysis data are used to establish an HGE model, variations in S1 and S2 content are used to assess hydrocarbon generation and expulsion. As the degree of thermal evolution increases, S2 will continue to decrease by converting to S1, which will undergo an expulsion process exhibiting an increase followed by a decrease. If there is a loss of S1 and S2 is overestimated, a significant effect is that it leads to an underestimation of the proportion of S2 to S1 conversion, i.e., TR. In addition, the loss of S1 also leads to an underestimation of hydrocarbon generation,

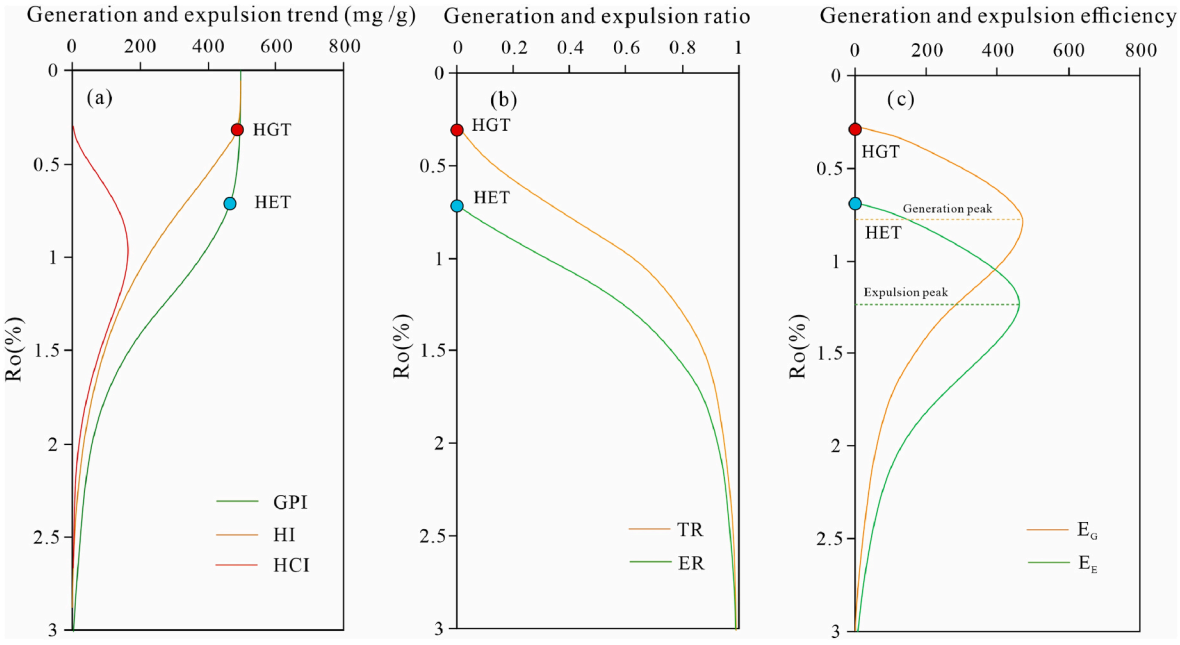

Fig. 14. HGE model of Es_3^M in the northern Dongpu Depression. (a) HGE trend, (b) HGE ratio. (c) HGE efficiency.

which implies that the HGT may be recognised at a higher maturity stage (where more hydrocarbons are generated), whereas a decrease in S1 due to loss of S1 in the oil-window stage makes it possible that the HET may be incorrectly identified.

Vandenbroucke and Largeau (2007) reviewed kerogen evolution and classification and showed that hydrocarbon potential of kerogen is demonstrated to show the order of Type I > Type II > Type III. Therefore, there may be some differences in the HGE models of shales with different kerogen types. Maturity affects the hydrocarbon TR and ER. This model used Ro to simulate the HGE process. When Ro is <0.37 %, there is no hydrocarbon generation. When Ro reaches 1.6 %, the HGE potential is lower. Further, when Tmax is used to represent maturity for modelling purposes, the equation for Tmax versus Ro should be established. It is important to note that Tmax is affected by hydrocarbon migration, type of kerogen and S2, and a datasets with strong similarity and removal of anomalies should be used to build the bridge (Espitalié, 1986; Peters, 1986; Katz and Lin, 2021). Especially when maturity is high, S2 may be relatively low and affect the accuracy of Tmax.

5.2. *Effect of hydrocarbon micromigration on hydrocarbon resource distribution*

Hydrocarbons enter in tight reservoir due to the close-distance migration of hydrocarbons expelled from shale or remain in shale reservoirs due to retention and micromigration (Pang et al., 2005). Two types of small-scale migration processes occur in organic-rich layers: migration of expelled hydrocarbons from shale to tight interlayers and that of hydrocarbons generated by organic-rich lamina to organic-poor lamina (Zhang et al., 2021), which implies that the spatial assemblage relationship between the micro-source and micro-storage shales is important for the migration of hydrocarbons, and that structures with a high frequency of interlayers will be more active in migration (Raji et al., 2015). In particular, high-quality micro-reservoirs provide storage space for migrating hydrocarbons, while high-quality micro-source rocks not only generate hydrocarbons but also create breakthrough pressure between source and reservoir, which serves as a key driving force for hydrocarbon migration (Mackenzie et al., 1988; Hunt, 1990; Cui et al., 2022). Shale with high hydrocarbon expulsion potential can lead to low hydrocarbon content, while shale with low hydrocarbon generation potential can contribute to high hydrocarbon content due to accept external hydrocarbons. Neglecting the presence of migrating hydrocarbons greatly deteriorates hydrocarbon modeling accuracy.

From the vertical distribution of samples, the following information was obtained (Fig. 15): (1) samples that receive and expel hydrocarbons tend to be closely distributed, indicating that migration is prevalent over short distances. What is certain is that migration of shale oil on millimeter-centimeter scale is very common (Fig. 11); (2) samples that receive a large amount of external hydrocarbons generally have high light-hydrocarbon content, high nonclay mineral content, and high mobility and their HI_0 and OSI values generally do not match; (3) samples that expell a large amount of hydrocarbons generally have high organic matter contents and HI_0 values, high clay mineral content; and (4) tight sandstone with good oil-bearing properties often are observed adjacent to shale, and its migration can be up to 5–10m. In organic-rich layers, segments with high hydrocarbon reception develop shale reservoirs with frequent interlayers, best mobility, and moderate oil-bearing properties. Segments with high hydrocarbon expulsion shale reservoirs in the nearby area usually close tight sandstone reservoirs, with moderate mobility, and best oil-bearing properties.

5.3. *Factors influencing the HGE trend and hydrocarbon resource*

After organic-rich rocks undergo HGE, HI and GPI decrease with increasing thermal maturity, with the evolution trends represent the hydrocarbon generation kinetics of different kerogens (Tissot and Espitalié, 1975; Pang et al., 2005; Chen et al., 2015). The envelope line around data are mainly used to determine the HGE path (Fig. 2a), and the envelope lines consider only the maximum hydrocarbon generation amounts, which clearly overestimates the resource potential. When using pyrolysis data combined with hydrocarbon generation dynamics for resource assessment, the data points should cover the entire range of hydrocarbon generation temperatures. Missing data are likely to affect the accuracy of HGE trend identification. For example, lack of low-maturity samples in the Longmaxi Formation shale in the Sichuan Basin makes it difficult to determine GPI_0. In contrast, shale used in this study lacked high-maturity samples, making it difficult to confirm the HGE endpoint. Formulations based on hydrocarbon generation kinetics constrain the trend of shale HGE (Equation (4), Equation (11)), and the use of Monte Carlo simulation combined with limited pyrolysis data can effectively solve this problem. Other factors influencing the calculation

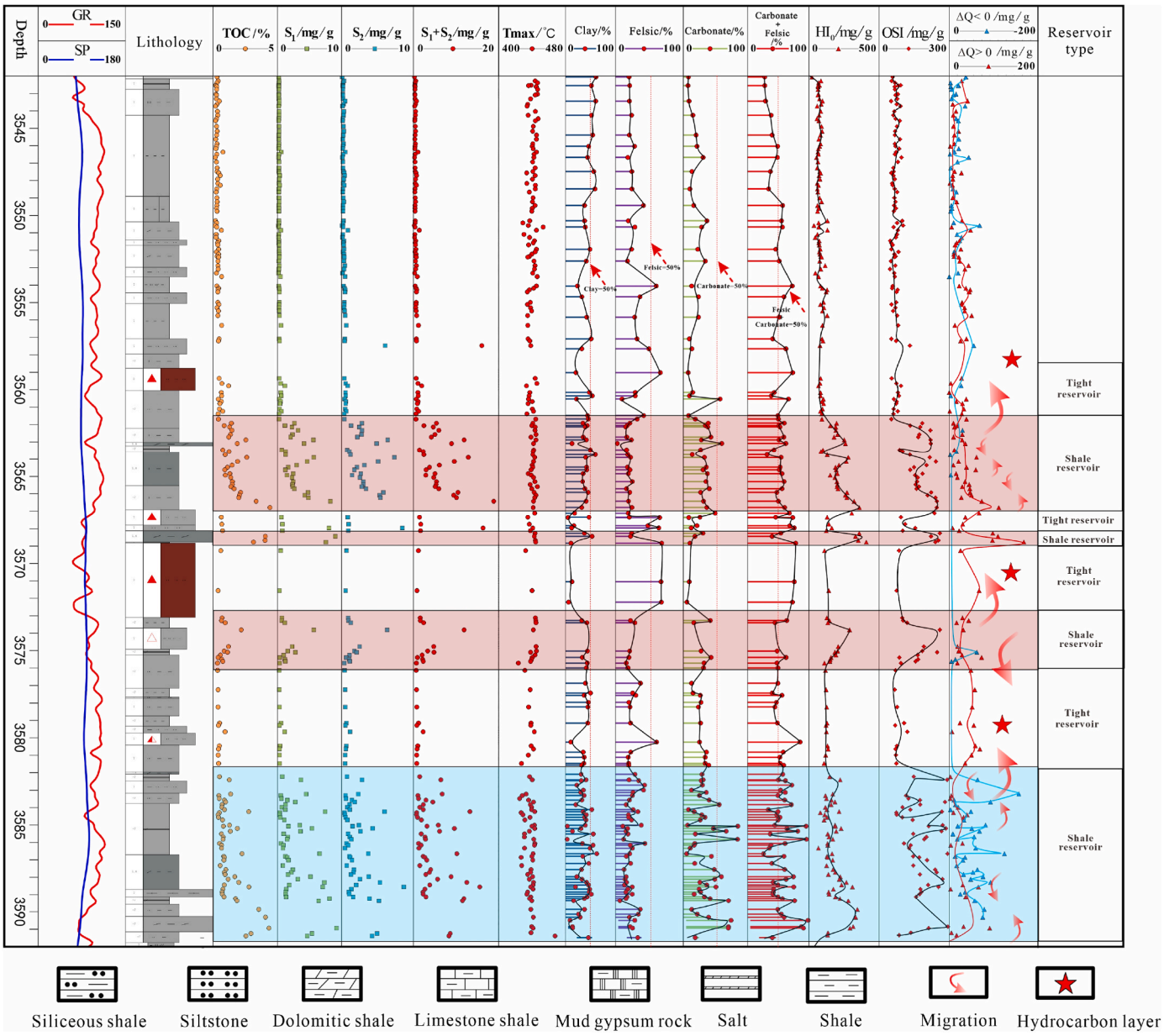

Fig. 15. Comprehensive geochemical profile of Es_3^M shales in well W410 obtained from the northern Dongpu Depression.

of the HGE potential include the thickness, density, and area of organic-rich rocks as well as the HI_0 and TOC values. Generally, resource evaluation is performed by overlaying the distribution maps of various parameters for each stratigraphic interval. However, the mass of rock loss and organic matter during HGE significantly affect these parameters.

The current TOC distribution in the Dongpu Depression is within the range of 0.15 %–7.76 %, with an average of 1.26 %. As the hydrocarbons in the organic-rich rock are expelled, the mass and TOC of rock decreases with increasing thermal maturity, with a maximum mass loss of up to 6 % (Fig. 16a). The initial TOC_0 value can range from 0.25 % to 12.12 %. The source rock has lost approximately half of its original TOC value (Fig. 16b). For the purpose of calculation, a rock density and thickness of 2.5 g/cm^3 and 100 m is assumed, respectively, and as the thermal alteration progresses to the current stage (0.8 %–1.2 % Ro), the corresponding hydrocarbon TR and ER values are 0.42–0.77 (0.60) and 0.14–0.54 (0.34), respectively. Under these conditions, the effects of TOC_0 and G_0 are analyzed on the HGE potential of shales for different TOC values and found that the HGE potential was significantly underestimated before correction, especially for high-abundance, high-maturity shales; the maximum HGE intensity may have been underestimated by >20 % (Table 1).

5.4. *Significance of the proposed method for hydrocarbons exploration*

Unlike conventional hydrocarbons that accumulate in high porosity and permeability reservoirs, shale hydrocarbons accumulate within the low permeability source and are widely distributed (Tissot and Espitalié, 1975; Jarvie, 2012; Curtis, 2002). Previous studies have shown that the residual-hydrocarbon content in shales in the Bohai Bay Basin is ~54 %, while the content of expelled hydrocarbons in conventional and tight reservoirs are ~11 % and 35 %, respectively (Fig. 17a), which is based on the understanding that expelled hydrocarbons can only migrate into reservoirs such as sandstone (Pang et al., 2020). However, the results of the micromigration evaluation showed that more than 59 % of the expelled hydrocarbons remained in the shale and its interlayers, which indicating that the shale hydrocarbon content is larger than that previously assumed. Combining these two results, 59 % of the amount of tight

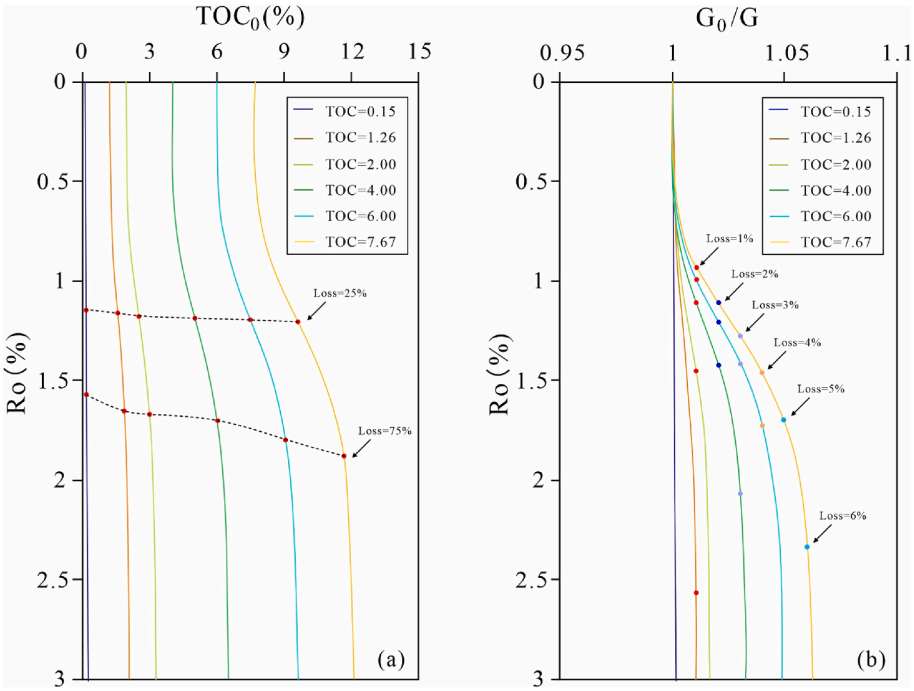

Fig. 16. Sensitivity analysis of TOC and G_0 of Es_3^M shale in the northern Dongpu Depression.

Table 1
Comparison of the HGE characterization before and after calibration of TOC_0 and G_0.

TOC (%)	Ro (%)	I_g (10^4 t/km^2)	I_g before calibration (10^4 t/km^2)	I_e (10^4 t/km^2)	Ie before calibration (10^4 t/km^2)
0.15	0.8–1.2	8.2–17.9	7.7–14.2	2.7–12.6	2.6–9.9
1.26		68.9–151.9	64.8–118.9	22.98–106.5	21.6–83.4
2		109.1–242.0	102.9–188.7	36.4–169.7	34.3–132.3
4		217.6–481.1	205.8–377.3	72.5–337.4	68.6–264.6
6		326.2–724.5	308.7–566.0	108.7–508.1	102.9–396.9
7.76		416.8–929.8	399.3–732.0	138.9–652.1	133.1–513.3

and conventional hydrocarbons should belong to shale hydrocarbons. In summary, it was was determined that shale hydrocarbons account for 81.1 %, tight hydrocarbons account for 14.4 %, and conventional hydrocarbons account for 4.5 % of the generated hydrocarbons (Fig. 17b). Zhu et al. (2021) calculated that the amount of hydrocarbons expelled from the Es_3^M of the Dongpu Depression was 2.662 billion tons. Based on the 59 % proportion of expelled hydrocarbons, the calculated shale hydrocarbon resources are estimated at 1.57 billion tons. Because this part of shale hydrocarbon has experienced migration, its mobility may be better than other residual shale hydrocarbon mobility. Based on the above hydrocarbon residues and expulsions, it can know that: (1) conventional hydrocarbons are the easiest to explore, but they are present in small quantities; (2) tight hydrocarbons have moderate mobility, and their quantities are also moderate; (3) shale hydrocarbons occur in the largest quantities. Expelled hydrocarbons that remain in shale formations migrate into mixed shale or interlayers shale. Shale includes hydrocarbons remaining in the shale interlayer after micromigration, in addition to those remaining after hydrocarbon expulsion.

5.5. Shortcomings of the developed method and directions for improvement

A comprehensive calculation process for shale, tight, and conventional primary hydrocarbons is presented, which benefits the estimation and exploration of hydrocarbon resources. This method is particularly advantageous as a preliminary reference during the early stages of exploration. As exploration progresses and methods are combined, the uncertainty is reduced. Additionally, this method enables the estimation of original hydrocarbon volumes, which, after appropriate conversion, may serve as a more effective constraint on the upper limit of resource potential. Despite efforts to refine the workflow of this method, there is potential for improvement. First, this study presents only a preliminary workflow. Lacustrine shale exhibits heterogeneity in terms of kerogen type, structure (block or laminate) (Katz, 1990, 1995; Katz and Lin, 2014), and sedimentary environment, which may lead to slight variations in the HGE model. Future research could enhance comparison of the above parameters. Second, the removal of anomalous low rock pyrolysis values was based on empirical values. In the future, with the generation of large datasets, machine learning methods can be used for data filtering and classification to develop more reliable models. Third, this study provides a simple and quick workflow to determine the micromigration threshold ($\Delta Q < 6$ % of HI_0). In actual scenarios, organic-rich rocks contain section where hydrocarbons are not received or expelled, suggesting the need to develop more accurate threshold identification methods. Finally, the confidence intervals of hydrocarbon resources profoundly influence exploration decisions. This method provides a classification scheme for three types of primary hydrocarbons: retained hydrocarbons, expelled conventional hydrocarbons, and expelled tight hydrocarbons. In the future, the three hydrocarbon types can be combined with geological conditions to categorize different resource levels, such as current recoverable resources, potential resources, and prospective resources. For example, the thickness, physical properties and mineral composition of the reservoir, the quality and scale of the trap and migration channels, and the preservation conditions at a later stage will significantly affect how much of the hydrocarbons generated can be accumulated and preserved, and how much of it can be extracted. Although there is potential for improvement in this method, it is believed that it provides a a foundation for future for researchers.

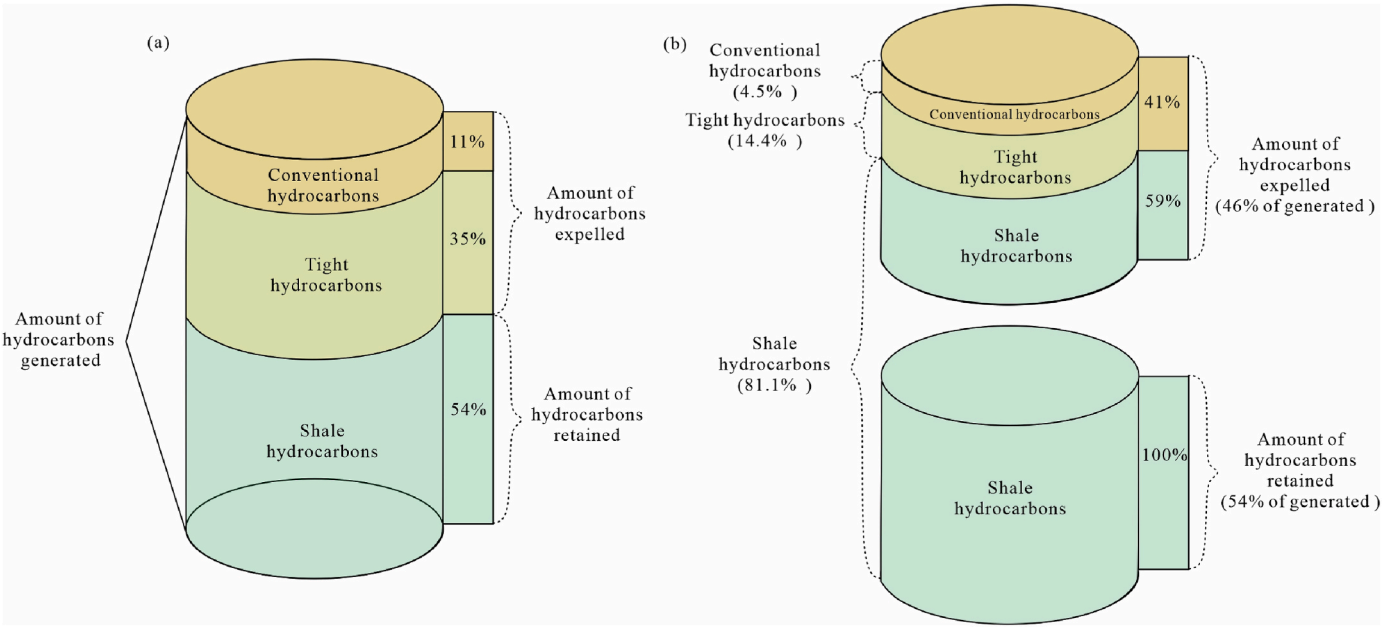

Fig. 17. Relative proportions of conventional, tight, and shale hydrocarbons (a) Original relative proportions. (b) Relative proportions corrected for micromigration evaluation results.

6. Conclusion

Herein, a method for hydrocarbon resource evaluation is developed and applied to the Es_3^M in the northern Dongpu Depression. Many of the samples of the shale do not serve as effective source rocks, leading to a reconsideration of the hydrocarbon generation and storage capacity.

(1) An effective source rock should be a shale that is capable of expelling hydrocarbons, and its share in our study is 62 %. The average GPI_0 of organic-rich rocks was 490 mg/g, with an HGT and HET of 0.37 % and 0.68 % Ro.
(2) Conventional pyrolysis have led to an S1 loss reaching up to 53 %. Neglecting the mass and TOC loss of organic-rich rock could make the resource underestimatation greater than 20 %.
(3) 59 % of the expelled hydrocarbons remain trapped within the shale sequence, while the remaining portion migrates into other reservoirs. The generated hydrocarbons are distributed 81.1 % in shale, 14.4 % in tight sandstones reservoirs, and 4.5 % in conventional reservoirs. Hydrocarbon volumes in shale sequence are larger than traditionally thought.

CRediT authorship contribution statement

Huiyi Xiao: Writing – review & editing, Writing – original draft, Methodology, Investigation, Data curation. **Tao Hu:** Supervision, Methodology, Funding acquisition, Formal analysis. **Xiongqi Pang:** Supervision, Methodology, Conceptualization. **Yunlong Xu:** Writing – review & editing, Data curation. **Yao Hu:** Writing – review & editing, Methodology. **Caijun Li:** Software, Data curation. **Tianwu Xu:** Writing – review & editing, Data curation. **Dingye Zheng:** Writing – review & editing, Methodology. **Tingyu Pu:** Software, Methodology. **Chenxi Ding:** Visualization, Software. **Zhiming Xiong:** Visualization, Software. **Shu Jiang:** Investigation, Formal analysis. **Kanyuan Shi:** Software, Formal analysis. **Qinglong Lei:** Software, Investigation. **Yuqi Wu:** Writing – review & editing. **Maowen Li:** Writing – review & editing.

Declaration of competing interest

The authors declare that they have no known competing financial interests or personal relationships that could have appeared to influence the work reported in this paper.

Acknowledgments

This study was financially supported by the National Natural Science Foundation of China (U22B6004, 42202133, U24B6002), CNPC Innovation Fund (2022DQ02-0106), Key Laboratory of Tectonics and Petroleum Resources of the Ministry of Education (TPR-2023-05), National Natural Science Foundation of China (41872148, 42072174, 42130803), Strategic Cooperation Technology Projects of the CNPC and CUPB (ZLZX2020-01-05), Sinopec Zhongyuan Oilfield and CUPB Cooperation Project (31300027-23-ZC0613-0013), AAPG Foundation Grants-in-Aid Program (22272306).

Appendices A. Formula

Hydrocarbon expulsion and generation rate efficiency (f) can be expressed as:

$$f = \frac{ER}{TR} \tag{A1}$$

Hydrocarbon generation efficiency (E_G) can be expressed as:

$$E_{G(Ro)} = -HI(Ro)^{-1} \tag{A2}$$

Hydrocarbon expulsion efficiency (E_E) can be expressed as:

$$E_{E(Ro)} = -GPI(Ro)^{-1} \tag{A3}$$

Generation intensity (I_g) can be expressed as:

$$I_g = \int 10^{-3} \times HI_0 \times \mathrm{TOC}_0 \times \rho \times \mathrm{H} \times \phi \times TR \times d(Ro) \tag{A4}$$

Expulsion intensity (I_e) can be expressed as:

$$I_e = \int 10^{-3} \times \mathrm{GPI}_0 \times \mathrm{TOC}_0 \times \rho \times \mathrm{H} \times \phi \times ER \times d(Ro) \tag{A5}$$

Residual intensity (I_r) can be expressed as:

$$I_r = \int 10^{-3} \times \mathrm{HI}_0 \times \mathrm{TOC}_0 \times \rho \times \mathrm{H} \times \phi \times (TR - ER) \times d(Ro) \tag{A6}$$

Hydrocarbon generation quantity (Q_g) can be expressed as:

$$Q_g = \iint 10^{-3} \times \mathrm{HI}_0 \times \mathrm{TOC}_0 \times \rho \times \mathrm{H} \times \phi \times TR \times d(Ro) \times d(S) \tag{A7}$$

Hydrocarbon expulsion quantity (Q_e) can be expressed as:

$$Q_e = \iint 10^{-3} \times \mathrm{GPI}_0 \times \mathrm{TOC}_0 \times \rho \times \mathrm{H} \times \phi \times ER \times d(Ro) \times d(S) \tag{A8}$$

Residual hydrocarbon quantity (Q_r) can be expressed as:

$$Q_r = \iint 10^{-3} \times \mathrm{GPI}_0 \times \mathrm{TOC}_0 \times \rho \times \mathrm{H} \times \phi \times (TR - ER) \times d(Ro) \times d(S) \tag{A9}$$

Data availability

Data will be made available on request.

References

Barker, C.E., Pawlewicz, M.J., 1993. An empirical determination of the minimum number of measurements needed to estimate the mean random vitrinite reflectance of disseminated organic matter. Org. Geochem. 20 (6), 643–651.

Burnham, A.K., 1989. On the validity of the pristane formation index. Geochem. Cosmochim. Acta 53 (7), 1693–1697.

Chen, Z.H., Jiang, C.Q., 2015. A data driven model for studying kerogen kinetics with application examples from Canadian sedimentary basins. Mar. Petrol. Geol. 67, 795–803.

Chen, Z.H., Li, M.W., Jiang, C.Q., Qian, M.H., 2019. Shale oil resource potential and its mobility assessment: a case study of Upper Devonian Duvernay shale in Western Canada sedimentary Basin. Oil Gas Geol. 40 (3), 459–468 (in Chinese with English abstract).

Clementz, D.M., 1979. Effect of oil and bitumen saturation on source-rock pyrolysis: geologic notes. AAPG Bull. 63 (12), 2227–2232.

Cui, J.W., Zhang, Z.Y., Liu, G.L., Zhang, Y., Qi, Y.L., 2022. Breakthrough pressure anisotropy and intra-source migration model of crude oil in shale. Mar. Petrol. Geol. 135, 105433.

Curtis, J.B., 2002. Fractured shale - gas systems. AAPG Bull. 86 (11), 1921–1938.

Delvaux, D., Martin, H., Leplat, P., Paulet, P., 1990. Comparative rock-eval pyrolysis as an improved tool for sedimentary organic matter analysis. Org. Geochem. 16, 1221–1229.

Espitalie, J., 1986. Use of Tmax as a maturation index for different types of organic matter comparison with vitrinite reflectance. In: Burrus, J. (Ed.), Thermal Modeling in Sedimentary Basins. Editions Technip, Paris, pp. 475–496.

Gao, Z.Y., Duan, L.F., Jiang, Z.X., Huang, L.L., Chang, J.Q., Zheng, G.W., Wang, Z.W., An, F., Wei, W.H., 2023. Using laser scanning confocal microscopy combined with saturated oil experiment to investigate the pseudo in-situ occurrence mechanism of light and heavy components of shale oil in sub-micron scale. J. Petrol. Sci. Eng. 220, 111234.

Hackley, P.C., Zhang, T.W., Jubb, A.M., Valentine, B.J., Dulong, F.T., Hatcherian, J.J., 2020. Organic petrography of Leonardian (Wolfcamp A) mudrocks and carbonates, Midland Basin, Texas: the fate of oil-prone sedimentary organic matter in the oil window. Mar. Petrol. Geol. 112, 104086.

Han, Y.J., Mahlstedt, N., Horsfield, B., 2015. The Barnett Shale: compositional fractionation associated with intraformational petroleum migration, retention, and expulsion. AAPG Bull. 99 (12), 2173–2202.

Hu, T., Jiang, F.J., Pang, X.Q., Liu, Y., Wu, G.Y., Zhou, K., Xiao, H.Y., Jiang, Z.X., Li, M. W., Jiang, S., Huang, L.L., Chen, D.X., Meng, Q.Y., 2024. Identification and evaluation of shale oil micro-migration and the petroleum geological significance. Petrol. Explor. Dev. 51 (1), 1–13.

Hu, T., Jing, Z.H., Zhang, Q., Pan, Y, Yuan, M., Li, M.W., 2025. Shale oil micro-migration characterization: Key methods and outlook. Adv. Geo-Energy Res. 15 (1), 5–12.

Hu, T., Liu, Y., Jiang, F.J., Pang, X.Q., Wang, Q.F., Zhou, K., Wu, G.Y., Jiang, Z.X., Huang, L.L., Jiang, S., Zhang, C.X., Li, M.W., Chen, Z.X., 2023. A Novel Method for Quantifying Hydrocarbon Micromigration in Heterogeneous Shale and the Controlling Mechanism.Energy, 129712.

Hu, T., Pang, X.Q., Jiang, S., Wang, Q.F., Zheng, X.W., Ding, X.G., Zhai, Y., Zhu, C.X., Li, H., 2018. Oil content evaluation of lacustrine organic-rich shale with strong heterogeneity: a case study of the middle Permian Lucaogou formation in Jimusaer Sag, Junggar Basin, NW China. Fuel 221, 196–205.

Hu, T., Pang, X.Q., Xu, T.W., Li, C.R., Jiang, S., Wang, Q.F., Chen, Y.Y., Zhang, H.A., Huang, C., Gong, S.Y., Gao, Z.C., 2022. Identifying the key source rocks in heterogeneous saline lacustrine shales: paleogene shales in the Dongpu depression, Bohai Bay Basin, eastern China. AAPG Bull. 106 (6), 1325–1356.

Hunt, J.M., 1990. Generation and migration of petroleum from abnormally pressured fluid compartments. AAPG Bull. 74 (1), 1–12.

IEA, 2023. World Energy Outlook 2023.2023.Paris:IEA.

Jarvie, D.M., 2012. Shale resource systems for oil and gas: part 2-shale-oil resource systems. In: Breyer, J.A. (Ed.), AAPG Mem, vol. 97, pp. 89–119.

Jarvie, D.M., 2014. Components and processes affecting producibility and commerciality of shale resource systems. Geol. Acta 12 (12), 307–325, 2014.

Ji, H., Li, S.M., Greenwood, P., Zhang, H.A., Pang, X.Q., Xu, T.W., He, N.N., Shi, Q., 2018. Geochemical characteristics and significance of heteroatom compounds in lacustrine oils of the Dongpu depression (Bohai Bay Basin, China) by negative-ion Fourier transform ion cyclotron resonance mass spectrometry. Mar. Petrol. Geol. 97, 568–591.

Jia, C.Z., 2017. Breakthrough and significance of unconventional oil and gas to classical petroleum geological theory. Petrol. Explor. Dev. 44 (1), 1–11.

Jiang, H., Pang, X.Q., Shi, H.S., Yu, Q.H., Cao, Z., Yu, R., Chen, D., Long, Z.L., Jiang, F.J., 2015. Source rock characteristics and hydrocarbon expulsion potential of the middle Eocene Wenchang formation in the Huizhou depression, Pearl River Mouth basin, South China Sea. Mar. Petrol. Geol. 67, 635–652.

Jiang, Q.G., Li, M.W., Qian, M.H., Li, Z.M., Li, Z., Huang, Z.K., Zhang, C.M., Ma, Y.Y., 2016. Quantitative characterization techniques and applications of shale oil in different occurrence states. Petroleum Geology & Experiment 6, 842–849 in Chinese with English abstract.

Jubb, A.M., Hackley, P.C., Hatcherian, J.J., Qu, J., Nesheim, T.O., 2019. Nanoscale molecular fractionation of organic matter within unconventional petroleum source beds. Energy Fuels 33 (10), 9759–9766.

Katz, B.J., 1990. Controls on distribution of lacustrine source rocks through time andspace. In: Katz, B.J. (Ed.), Lacustrine Basin Exploration: Case Studies and ModernAnalogs, AAPG Mem, vol. 50, pp. 61–76.

Katz, B.J., 1995. Factors controlling the development of lacustrine petroleum sourcerocks-an update. AAPG studies in geology, no. 40. In: Huc, A.Y. (Ed.), Paleogeography, Paleoclimate, and Source Rocks. AAPG, Tulsa, pp. 61–79.

Katz, B.J., Lin, F., 2014. Lacustrine basin unconventional resource plays: key differencesMar. Pet. Geol. 56, 255–265.

Katz, B.J., Lin, F., 2021. Consideration of the limitations of thermal maturity with respect to vitrinite reflectance, Tmax, and other proxies. AAPG Bull. 105 (4), 695–720.

Lehne, E., Dieckmann, V., 2007. Bulk kinetic parameters and structural moieties of asphaltenes and kerogens from a Sulphur-rich source rock sequence and related petroleums. Org. Geochem. 38, 1657–1679.
Li, C.R., Pang, X.Q., Huo, Z.P., Wang, E.Z., Xue, N., 2020. A revised method for reconstructing the hydrocarbon generation and expulsion history and evaluating the hydrocarbon resource potential: example from the first member of the Qingshankou formation in the Northern Songliao Basin, Northeast China. Mar. Petrol. Geol. 121, 104577.
Li, M.W., Chen, Z.H., Cao, T.T., Ma, X.X., Liu, X.J., Li, Z.M., Jiang, Q.G., Wu, S.Q., 2018. Expelled oils and their impacts on rock-eval data interpretation, Eocene Qianjiang formation in Jianghan Basin, China. Int. J. Coal Geol. 191, 37–48.
Li, S.M., Ji, H., Wan, Z.H., Pang, X.Q., Zhang, H.A., Xu, T.W., Zhou, Y.S., 2021. Geochemical characteristics and factors controlling the deep lithologic reservoirs in Puwei Sag, Dongpu depression—A case study of well PS20. J. Petrol. Sci. Eng. 203, 108669.
Mackenzie, A.S., Leythaeuser, D., Muller, P., Quigley, T.M., Radke, M., 1988. The movement of hydrocarbons in shales. Nature 331 (6151), 63–65.
Magoon, L.B., Dow, W.G., 1991. The petroleum-system from source to trap. AAPG Bull. 1991, 75.
Masters, J.A., 1979. Deep Basin gas trap, Western Canada. AAPG Bull. 63 (2), 152–181.
Pang, X.Q., Jia, C.Z., Chen, J.Q., Li, M.W., Wang, W.Y., Hu, Q.H., Guo, Y.C., Chen, Z.X., Peng, J.W., Liu, K.Y., Wu, K.L., 2020. A unified model for the formation and distribution of both conventional and unconventional hydrocarbon reservoirs. Geosci. Front. 12 (2), 695–711.
Pang, X.Q., Jia, C.Z., Wang, W.Y., Chen, Z.X., Li, M.W., Jiang, F.J., Hu, T., Wang, K., Wang, Y.X., 2021. Buoyance-driven hydrocarbon accumulation depth and its implication for unconventional resource prediction. Geosci. Front. 12 (4), 101133.
Pang, X.Q., Li, M.W., Li, S.M., Jin, Z.J., 2005. Geochemistry of petroleum systems in the Niuzhuang south slope of Bohai Bay Basin: part 3. Estimating petroleum expulsion from the Shahejie formation. Org Geochem 36, 497–510.
Patidar, A.K., Singh, R.K., 2024. A systematic approach for planning a geochemical survey for hydrocarbon exploration: an overview. Ir. J. Earth Sci. 6 (2), 1–9, 162408.
Peters, K.E., 1986. Guidelines for evaluating petroleum source rock using programmed pyrolysis. AAPG Bull. 70 (3), 318–329.
Raji, M., Gröcke, D.R., Greenwell, H.C., Gluyas, J.G., Cornford, C., 2015. The effect of interbedding on shale reservoir properties. Mar. Petrol. Geol. 67, 154–169.
Tissot, B.P., Espitalié, J., 1975. Thermal evolution of organic-matter in sediments-application of a mathematical simulation-petroleum potential of sedimentary basins and reconstructing thermal history of sediment. Rev. Inst. Fr. Petrol 30 (5), 743–778.
Tu, J.Q., Li, P., 2012. Oil and Gas Industry Standard of the People's Republic of China: Method of Determining Microscopically the Reflectance of Vitrinite in Sedimentary (SY/T 5124–2012). Petroleum Industry Press, Beijing.
U.S. Geological Survey, 2012. USGS World Petroleum Assessment 2012. U.S. Department of the Interior.
Vandenbroucke, M., Largeau, C., 2007. Kerogen origin, evolution and structure. Org. Geochem. 38 (5), 719–833.
Wang, E.Z., Li, C.R., Feng, Y., Song, Y.C., Guo, T.L., Li, M.W., Chen, Z.H., 2022. Novel method for determining the oil moveable threshold and an innovative model for evaluating the oil content in shales. Energy 239, 121848.
Wang, M., Guo, Z.Q., Jiao, C.X., Lu, S.F., Li, J.B., Xue, H.T., Li, J.J., Li, J.Q., Chen, G.H., 2019. Exploration progress and geochemical features of lacustrine shale oils in China. J. Petrol. Sci. Eng. 178, 975–986.
Wang, M., Sherwood, N., Li, Z.S., Lu, S.F., Wang, W.G., Huang, A.H., Peng, J., Lu, K., 2015. Shale oil occurring between salt intervals in the Dongpu depression. Bohai Bay Basin, China: Int. J. Coal Geol. 152, 100–112.
White, David A., Gehman, Harry M., 1979. Methods of estimating oil and gas resources. AAPG Bull. 63 (12), 2183–2192.
Wu, L.Y., Zhang, Z.L., Yan, R.Q., Teng, Y.M., Li, B., Hu, S.L., 2012. National Standard of the People's Republic of China: Rock Pyrolysis Analysis (GB/T 18602–2012). Standard Press of China, Beijing.
Wu, Y.Q., Jiang, F.J., Hu, T., Xu, Y.L., Guo, J., Xu, T.W., Xin, H.L., Chen, D., Pang, H., Chen, J.Q., Zhu, C.X., 2024. Shale oil content evaluation and sweet spot prediction based on convolutional neural network. Mar Petro Geo 167, 106997.
Xu, G.J., Gao, Y., Dong, S.H., Wang, D.L., 2003. National Standard of the People's Republic of China: Determination of Total Organic Carbon in Sedimentary Rock (GB/T 19145–2003). Standard Press of China, Beijing.
Zeng, L., Wan, M.X., Li, X.H., Jiao, Y.G., Cui, S.N., Dong, X.D., Zhong, J., Qin, G.N., Wang, G.J., Yang, Q., Kuang, S.Y., Mao, S.H., 2018. Oil and Gas Industry Standard of the People's Republic of China: Analysis Method for Clay Minerals and Ordinary Non-clay Mineralsin Sedimentary Rocks by the X-ray Diffraction (SY/T 5163-2018). Petroleum Industry Press, Beijing.
Zeng, L.B., Su, H., Tang, X.M., Peng, Y.M., Gong, L., 2013. Fractured tight sandstone oil and gas reservoirs: a new play type in the Dongpu depression, Bohai Bay Basin, China. AAPG Bull. 97, 363–377.
Zhang, T.W., Fu, Q.L., Sun, X., Hackley, P.C., Ko, T.W., Shao, D.Y., 2021. Meter-scale lithofacies cycle and controls on variations in oil saturation, Wolfcamp A, Delaware and Midland Basins. AAPG Bull. 105 (9), 1821–1846.
Zheng, D.Y., Pang, X.Q., Ma, X.H., Li, C.R., Zheng, T.Y., Zou, L.M., 2019. Hydrocarbon generation and expulsion characteristics of the source rocks in the third member of the Upper Triassic Xujiahe formation and its effect on conventional and unconventional hydrocarbon resource potential in the Sichuan Basin. Mar. Petrol. Geol. 109, 175–192.
Zhu, C.X., Jiang, F.J., Zhang, P.Y., Hu, T., Liu, Y., Xu, T.W., Zhang, Y.X., Deng, Q., Zhou, Y.S., Xiong, H., Song, Z.Z., 2021. Identification of effective source rocks in different sedimentary environments and evaluation of hydrocarbon resources potential: a case study of paleogene source rocks in the Dongpu depression, Bohai Bay Basin. J. Petrol. Sci. Eng. 201, 108477.
Zou, C.N., Yang, Z., Zhang, G.S., Hou, L.H., Zhu, R.K., Tao, S.Z., Yuan, X.J., Dong, D.Z., Wang, Y.M., Guo, Q.L., Wang, L., Bi, H.B., Li, D.H., Wu, N., 2014. Conventional and unconventional petroleum "orderly accumulation": concept and practical significance. Petrol. Explor. Dev. 41 (1), 14–30.